DEC 23 1946

ACR No. L5F13a

NATIONAL ADVISORY COMMITTEE FOR AERONAUTICS

WARTIME REPORT

ORIGINALLY ISSUED
July 1945 as
Advance Confidential Report L5F13a

EFFECT OF LEAKAGE PAST AILERON NOSE ON AERODYNAMIC CHARACTERISTICS OF PLAIN AND INTERNALLY BALANCED AILERONS ON NACA 66(215)-216, a = 1.0 AIRFOIL

By J. D. Bird

Langley Memorial Aeronautical Laboratory
Langley Field, Va.

NACA

WASHINGTON

NACA WARTIME REPORTS are reprints of papers originally issued to provide rapid distribution of advance research results to an authorized group requiring them for the war effort. They were previously held under a security status but are now unclassified. Some of these reports were not technically edited. All have been reproduced without change in order to expedite general distribution.

L - 172

NATIONAL ADVISORY COMMITTEE FOR AERONAUTICS

ADVANCE CONFIDENTIAL REPORT

EFFECT OF LEAKAGE PAST AILERON NOSE ON AERODYNAMIC CHARACTERISTICS OF PLAIN AND INTERNALLY BALANCED AILERONS ON NACA 66(215)-216, a = 1.0 AIRFOIL

By J. D. Bird

SUMMARY

An investigation has been made in two-dimensional flow to determine the effect of leakage past the aileron nose on the aerodynamic characteristics of ailerons. Plain and internally balanced ailerons of 0.20 airfoil chord were tested on an NACA 66(215)-216, a = 1.0 airfoil. The effects of amount and type of leakage, aileron contour, and Mach number and Reynolds number were investigated.

The results of the tests indicated that a small amount of leakage area changed the pressure distributions over the plain and internally balanced ailerons markedly. This change generally resulted in negative increments in the lift and hinge-moment parameters c_{l_δ}, c_{h_α}, and c_{h_δ}. A further increase in the leakage area produced smaller changes in these parameters for the internally balanced aileron.

INTRODUCTION

Numerous investigations have been made in an attempt to develop ailerons with satisfactory hinge-moment characteristics. One of the most promising types yet devised and tested is the internally balanced aileron; however, installing and maintaining a complete seal across the entire aileron span, especially near the hinges, is rather difficult. It was therefore advisable to investigate the

effect of leakage past the balance plate on the characteristics of internally balanced ailerons. Several investigations have already been made with the nose gap unsealed and a correlation of some of the results is given in reference 1.

The present tests were made in an attempt to provide additional information on the characteristics of internally balanced ailerons and to determine whether a sufficient degree of balance can be maintained if the nose seal is eliminated. Because of the poor correlation of preliminary test results with existing data, it was found desirable to investigate the effects of Reynolds number and Mach number and the amount and type of leakage area on the characteristics of the internally balanced aileron. Tests were also made to determine the effect of an aileron-contour modification on the characteristics of the unsealed internally balanced aileron and the sealed and unsealed plain ailerons.

SYMBOLS AND DEFINITIONS

The coefficients and symbols used herein are defined as follows:

c_l airfoil section lift coefficient $\left(\frac{l}{qc}\right)$

c_h aileron section hinge-moment coefficient $\left(\frac{h}{qc_a^2}\right)$

l airfoil section lift

h aileron section hinge moment

c airfoil chord

c_a chord of aileron behind hinge axis

c_b chord of balance plate ahead of hinge axis

q free-stream dynamic pressure $\left(\frac{1}{2}\rho V^2\right)$

V free-stream velocity

ρ mass density of air

α_o angle of attack of airfoil for infinite aspect ratio

δ aileron angle with respect to airfoil

$c_{h_\alpha} = \left(\frac{\partial c_h}{\partial \alpha_o}\right)_\delta$ measured at $\alpha_o = 0^\circ$

$c_{h_\delta} = \left(\frac{\partial c_h}{\partial \delta}\right)_{\alpha_o}$ measured at $\delta = 0^\circ$

$c_{l_\alpha} = \left(\frac{\partial c_l}{\partial \alpha_o}\right)_\delta$ measured at $\alpha_o = 0^\circ$

$c_{l_\delta} = \left(\frac{\partial c_l}{\partial \delta}\right)_{\alpha_o}$ measured at $\delta = 0^\circ$

M Mach number (V/a)

a velocity of sound

P pressure coefficient $\left(\frac{p - p_o}{q}\right)$

p local static pressure on aileron or balance plate

p_o free-stream static pressure

The subscripts outside the parentheses of the parameters indicate the factors held constant.

The terms used herein are defined as follows:

Nose gap distance between nose of aileron or balance plate and adjoining wing (figs. 1 to 3)

Vent gap distance between aileron nose and balance shroud or cover plate (figs. 1 and 2)

End gap distance between end of balance plate and adjacent tunnel wall (fig. 3)

Equivalent nose gap — gap obtained by adding to nose gap the quotient of area at ends of balance plate divided by model span

Hinge gap — opening surrounding aileron hinge

APPARATUS AND TESTS

The tests were made in the two-dimensional test section of the Langley stability tunnel; this section is rectangular and is 6 feet high and $2\frac{1}{2}$ feet wide. Since the model, which is an NACA 66(215)-216, a = 1.0 airfoil section of 2-foot chord, completely spanned the width of the test section, two-dimensional flow was approximated. Table I gives the airfoil ordinates.

The 0.20c plain and internally balanced ailerons tested are shown in figures 1 to 3. A continuous flexible seal of cloth impregnated with plastic was used for the tests in which the nose gap was sealed. In all of the tests except that in which the aileron was completely sealed, there were gaps of approximately 0.001c between the ends of the balance plate and the tunnel walls. (See fig. 3.) For the completely sealed aileron, these end gaps as well as the nose gap were sealed. The vent gaps were unsealed for all tests. A concentrated leakage area simulating a hinge gap was obtained by sealing the nose gap completely and cutting a rectangular hole in the balance plate.

The airfoil and the aileron were mounted between two end disks that were rotated to change the angle of attack of the airfoil. Aileron hinge moments were measured with a spring balance. Lift was measured by an integrating manometer connected to orifices in the floor and ceiling of the tunnel. Pressures were measured through flush orifices installed at the center of the span of the aileron and balance plate. Table II gives the chordwise locations of these orifices.

All of the tests except the tests to determine the effect of varying the Reynolds number and Mach number were made at a test Mach number of 0.36, which corresponds

to a Reynolds number based on standard atmospheric conditions of approximately 5.1×10^6. The relation between Reynolds number for standard atmospheric conditions and test Mach number is shown in figure 4.

PRECISION OF TESTS

Angles of attack were set within $\pm 0.1^\circ$ and aileron angles within $\pm 0.3^\circ$. Check tests indicated that, at a Mach number of 0.36, values of c_h were accurate to within ± 0.003; c_l, within ± 0.01; and P, within ± 0.03.

Corrections for jet-boundary effects were applied to the lift coefficients and angles of attack. The corrected values were computed as follows:

$$c_l = 0.963\ c_{l_T}$$

$$\alpha_o = 1.023\ \alpha_{o_T}$$

where c_{l_T} and α_{o_T} are the uncorrected lift coefficient and angle of attack. No corrections were applied to the hinge-moment coefficients.

RESULTS AND DISCUSSION

Presentation of Data

Force-test data for the present report are given as section lift and aileron section hinge-moment coefficients plotted against aileron angle for a range of angle of attack or Mach number. The data for the sealed and unsealed true-contour plain ailerons are given in figure 5. Data for the internally balanced aileron with a constant vent gap of 0.010c and with end and nose gaps sealed are given in figure 6; with end gaps of 0.001c and nose gap sealed, in figure 7; and with end gaps of 0.001c and various nose gaps, in figure 8. Pressure distributions over the aileron and balance plate are given in figures 9 to 11. Results of tests of the internally balanced aileron with concentrated leakage area

for determining the effect of limiting the spanwise distribution of leakage past the balance plate are given in figure 12. Results of tests with reduced nose and vent gaps for determining whether the leakage area or the ratio of leakage area to vent area caused the greater part of the effects of leakage are given in figure 13. Data for the sealed and unsealed plain ailerons with straight sides are given in figure 14; for the unsealed internally balanced aileron with straight sides, in figure 15. The effect of Mach number and Reynolds number on the hinge-moment characteristics of the internally balanced aileron with leakage past the balance plate is given in figures 16 and 17.

Effect of Increased Leakage

Small aileron angles.- The values of c_{l_δ}, c_{h_α}, and c_{h_δ} for the plain and internally balanced ailerons are made more negative by increased leakage past the aileron nose or balance plate; the greater part of the change for the internally balanced aileron occurs for a small equivalent nose gap (fig. 18). The equivalent nose gap is obtained by adding to the nose gap the gap obtained by dividing the area at the ends of the balance plate by the span of the model. The value of c_{l_α} is little affected by increased leakage. An equivalent nose gap of 0.0002c, with the end gaps unsealed, caused the values of c_{h_δ} to become appreciably more negative. A comparison of the pressure distributions on the unsealed internally balanced aileron with the pressure distributions on the sealed internally balanced aileron (reference 2 and figs. 9 to 11) indicates that leakage past the balance plate produces a marked change in the pressure distribution on the aileron. This change in the pressure distribution, in addition to making the part of the aileron behind the hinge axis heavier and thus moving the center of pressure of the aileron nearer the aileron trailing edge, decreases the induced balancing pressure of the aileron. The curves of c_{h_δ} for various angles of attack indicate that small amounts of leakage past the balance plate are less critical at large angles of attack than at small angles of attack (fig. 18). For large amounts of leakage past the balance plate, the decrease in balancing pressure and the increase in heaviness of the part of the aileron behind the hinge axis become so

great that the unsealed internally balanced aileron becomes heavier - that is. has a more negative value of c_{h_δ} - than the plain sealed aileron.

The pressure distributions behind the hinge axis of the unsealed internally balanced aileron and the unsealed plain aileron show a marked similarity. This similarity is to be expected since the pressure distribution over the aileron surface is a function of the amount of leakage through the aileron as well as of angle of attack and aileron angle. For the unsealed plain and internally balanced ailerons compared in figures 9 and 10, the amount of leakage should be of the same order of magnitude because the nose gaps are equal.

Part of the leakage effect shown in the tests reported herein results from the existence of an extremely adverse pressure gradient near the trailing edge of the airfoil tested which, for a given amount of leakage, tends to cause separation farther forward on the airfoil than would be the case if a less adverse pressure gradient existed. Unpublished data on airfoils with a less adverse pressure gradient near the trailing edge have proved such airfoils to be less sensitive to leakage than the airfoil tested.

The internally balanced aileron tested is much more sensitive to leakage past the balance plate than the ailerons for which the correlation of reference 1 was made (fig. 19). The values of the balance ratio are more negative for the aileron tested than for the ailerons of the correlation curve for the range of leakage area shown in figure 19. It should be noted that most of the increase in heaviness (more negative value of c_{h_δ}) of the aileron tested occurs for small amounts of leakage area, whereas the increase in heaviness indicated by the correlation curve (reference 1) varies gradually with increase in leakage area. The sensitivity of the internally balanced aileron tested to small amounts of leakage area would make close aileron balance difficult without use of a complete nose seal.

Large aileron angles.- The slope of the curves of aileron hinge-moment coefficient against aileron angle for the unsealed internally balanced aileron (fig. 8) becomes less negative at large aileron angles and thereby indicates an increase in the degree of hinge-moment

balance. This trend is opposite that obtained for the usual aerodynamic balance. It should be noted that the aileron angle at which this increase occurs is a function of the angle of attack.

The change in the slope of the curves of hinge-moment coefficient at large aileron angles is caused by an abrupt increase in the rate of increase of balancing pressure (and thus of hinge-moment coefficient of the balance plate) with aileron angle as well as a positive increase in the value of c_{h_δ} of the plain unsealed aileron (fig. 20). The pressure distributions (figs. 9 to 11) indicate that the negative pressure causes the abrupt change in the slope of the curve of hinge-moment coefficient of the balance plate plotted against aileron angle.

Effect of Type of Leakage

A comparison of the hinge-moment characteristics of the aileron with concentrated leakage area at the midspan, of the aileron with the reduced nose and vent gaps, and of the aileron with the 0.005c nose gap and 0.010c vent gap is given in figure 21. All of these ailerons had approximately the same ratio of leakage area to vent area. Figure 21 shows that the aileron with the reduced nose and vent gaps has more closely balanced hinge-moment coefficients than the other two ailerons at large positive and negative aileron angles and has as close a degree of balance as either of the other two ailerons at small aileron angles. The aileron with the concentrated leakage area has less balance than either of the other two ailerons at both positive and negative aileron angles, except at very large aileron angles for which its degree of balance increases rapidly. This trend is similar to that of a control surface with plain overhang and hinge gaps as tested for reference 3. The hinge-moment characteristics of the internally balanced aileron with leakage past the balance plate generally were not changed radically by changing the leakage area from a narrow slit spanning the aileron at the balance-plate nose to a rectangular hole of about the same area located at the model midspan. The values of balance ratio for the ailerons with the concentrated leakage area and with the reduced nose and vent gaps are plotted in figure 19 against the ratio of leakage area to vent area.

Effect of Aileron-Contour Modification

The curves of c_h and c_l plotted against δ for the straight-sided plain and internally balanced ailerons (figs. 14 and 15) show the results to be expected from increasing the trailing-edge angle of the airfoil.

The value of balance ratio from the tests of the straight-sided aileron is plotted against the ratio of leakage area to vent area in figure 19. This value of the balance ratio was obtained by use of the values of c_{h_δ} for the straight-sided plain and internally balanced ailerons as determined from tests and the estimated value of c_{h_δ} for the sealed straight-sided internally balanced aileron. The value of c_{h_δ} for the sealed straight-sided internally balanced aileron was estimated by correcting the data for the sealed true-contour internally balanced aileron for the effect of the change in trailing-edge angle.

Effect of Mach Number and Reynolds Number

A comparison of figure 22 with data from reference 4 indicates that Mach number and Reynolds number have only slightly more effect on the values of c_{h_δ} for the unsealed internally balanced aileron than for the sealed internally balanced aileron. The variation of c_{h_δ} with Mach number and Reynolds number is in opposite directions for the angles of attack of 0° and 10.2°. These results indicate that, for the range of Mach number and Reynolds number tested (fig. 4), the effect of Mach number and Reynolds number on the values of c_{h_δ} was not appreciably different for sealed and unsealed internally balanced ailerons.

CONCLUSIONS

The effect of leakage past the aileron nose on the aerodynamic characteristics of plain and internally balanced ailerons on an NACA 66(215)-216, a = 1.0 airfoil has been investigated in two-dimensional flow. From the results of this investigation, the following conclusions have been reached:

1. A small amount of leakage area changed the pressure distributions over the plain and internally balanced ailerons markedly. This change generally resulted in negative increments in the lift and hinge-moment parameters c_{l_δ}, c_{h_α}, and c_{h_δ}. A further increase in the leakage area produced smaller changes in these parameters for the internally balanced aileron.

2. The sensitivity of the internally balanced aileron tested to small amounts of leakage area would make close aileron balance difficult without use of a complete nose seal.

3. The hinge-moment characteristics of the internally balanced aileron with leakage past the balance plate generally were not changed radically by changing the leakage area from a narrow slit spanning the aileron at the balance-plate nose to a rectangular hole of about the same area located at the model midspan.

4. Reducing the amount of leakage area and vent area so as to hold constant the ratio of leakage area to vent area increased the degree of hinge-moment balance at large aileron angles but caused no appreciable change in the degree of balance at small aileron angles.

5. The sealed and unsealed internally balanced ailerons had almost the same variation of c_{h_δ} with Mach number and Reynolds number.

Langley Memorial Aeronautical Laboratory
National Advisory Committee for Aeronautics
Langley Field, Va.

REFERENCES

1. Rogallo, F. M., and Lowry, John G.: Résumé of Data for Internally Balanced Ailerons. NACA RB, March 1943.

2. Letko, W., and Denaci, H. G.: Wind-Tunnel Tests of Ailerons at Various Speeds. V - Pressure Distributions over the NACA 66,2-216 and NACA 23012 Airfoils with Various Balances on 0.20-Chord Ailerons. NACA ACR No. 3K05, 1943.

3. Nivison, J.: Effect of Hinge Gaps on Control Characteristics. TN No. Aero 983 (Large Tunnel), British R.A.E., July 1942.

4. Denaci, H. G., and Bird, J. D.: Wind-Tunnel Tests of Ailerons at Various Speeds. II - Ailerons of 0.20 Airfoil Chord and True Contour with 0.60 Aileron-Chord Sealed Internal Balance on the NACA 66,2-216 Airfoil. NACA ACR No. 3F18, 1943.

TABLE I

ORDINATES FOR NACA 66(215)-216, a = 1.0 AIRFOIL

[Basic airfoil contour. Stations and ordinates in percent airfoil chord]

Upper surface		Lower surface	
Station	Ordinate	Station	Ordinate
0	0	0	0
.401	1.230	.599	-1.130
.640	1.484	.860	-1.344
1.128	1.858	1.372	-1.644
2.362	2.560	2.638	-2.188
4.846	3.604	5.154	-2.972
7.340	4.428	7.660	-3.580
9.838	5.140	10.162	-4.106
14.845	6.276	15.155	-4.930
19.860	7.156	20.140	-5.564
24.879	7.844	25.121	-6.054
29.900	8.366	30.100	-6.422
34.924	8.736	35.076	-6.676
39.949	8.980	40.051	-6.838
44.974	9.092	45.026	-6.902
50.000	9.060	50.000	-6.854
55.025	8.875	54.975	-6.685
60.048	8.496	59.952	-6.354
65.067	7.862	64.933	-5.802
70.081	6.941	69.919	-4.997
75.087	5.860	74.913	-4.070
80.085	4.644	79.915	-3.052
85.075	3.395	84.925	-2.049
90.055	2.103	89.945	-1.069
95.028	.913	94.972	-.281
100.000	0	100.000	0
L.E. radius: 1.575. Slope of radius through L.E.: 0.084			

NATIONAL ADVISORY
COMMITTEE FOR AERONAUTICS

TABLE II

CHORDWISE LOCATIONS OF ORIFICES FOR UNSEALED INTERNALLY BALANCED AILERON OF TRUE AIRFOIL CONTOUR

[Locations in percent aileron chord]

Location forward of hinge axis	Location behind hinge axis
72.3	4.2
66.8	11.5
56.7	32.3
45.7	68.8
23.0	89.6
12.5	----
4.2	----

NATIONAL ADVISORY
COMMITTEE FOR AERONAUTICS

UNCLASSIFIED

[redacted]

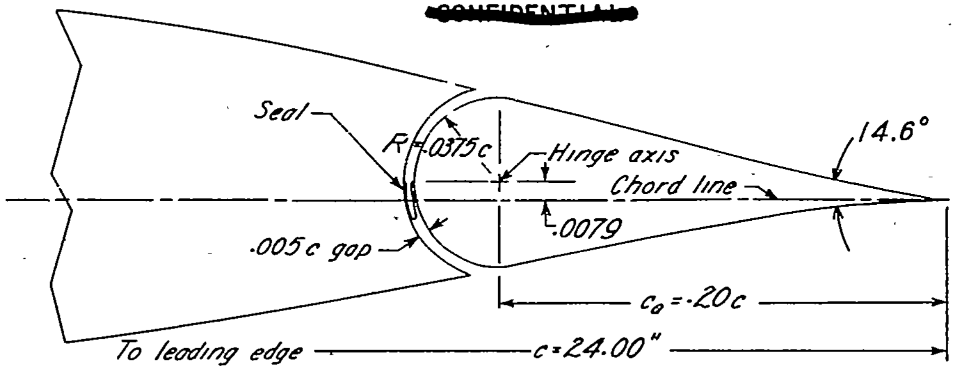

(a) Plain aileron, sealed or unsealed.

Variation of balance chord with nose gap	
Nose gap	c_b/c_a
0.0005c	0.766
.0015c	.761
.0030c	.754
.0050c	.744
.0100c	.719

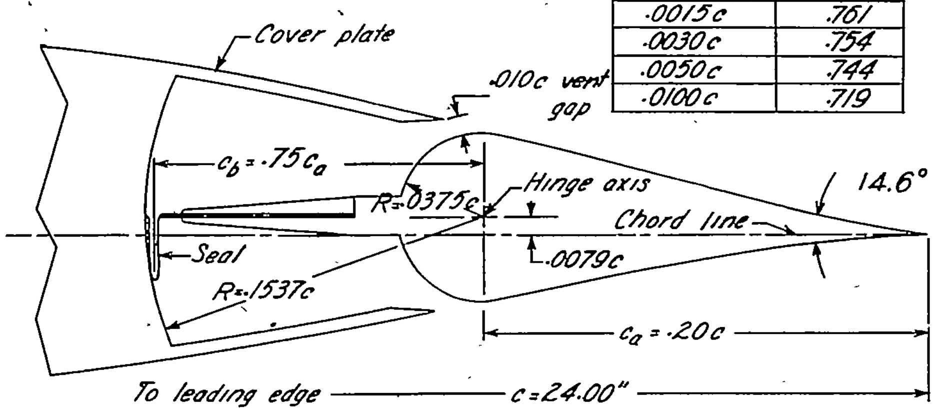

(b) Internally balanced aileron, sealed.

NATIONAL ADVISORY COMMITTEE FOR AERONAUTICS

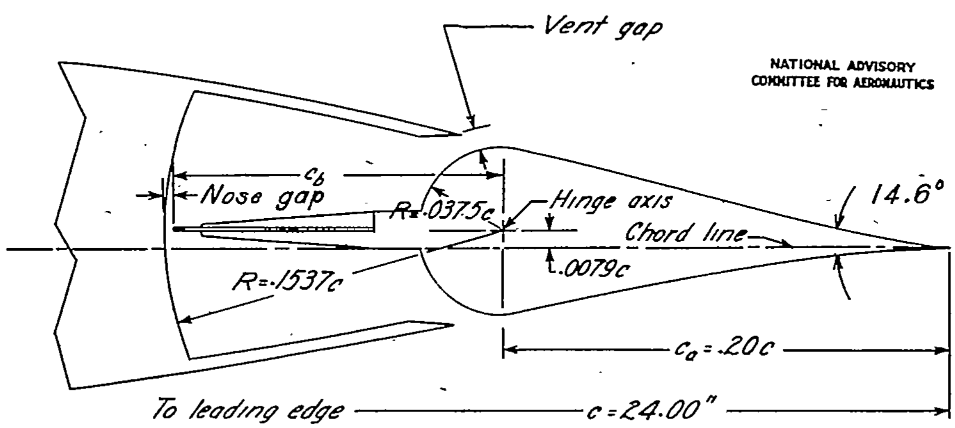

(c) Internally balanced aileron, unsealed.

Figure 1.- True-contour ailerons tested on NACA 66(215)-216, a=1.0 airfoil section. [redacted]

UNCLASSIFIED

UNCLASSIFIED

[redacted]

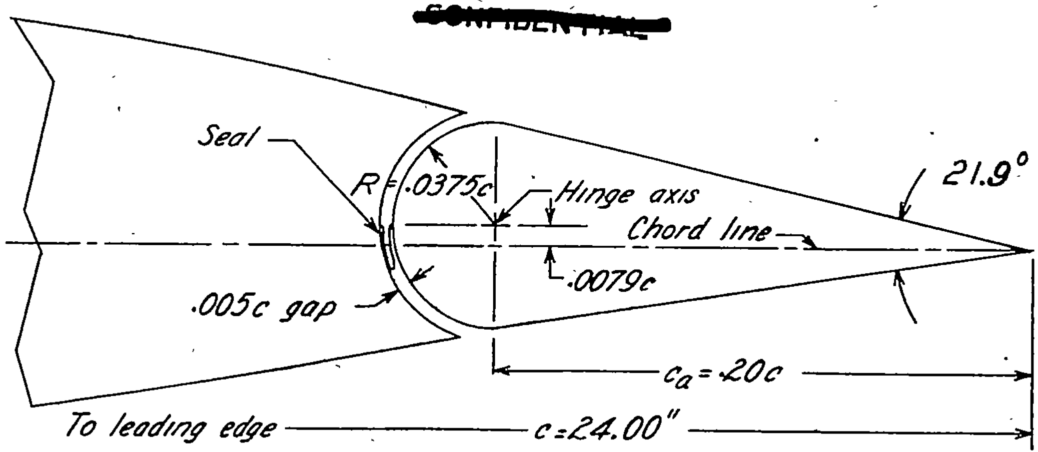

(a) Plain aileron, sealed or unsealed.

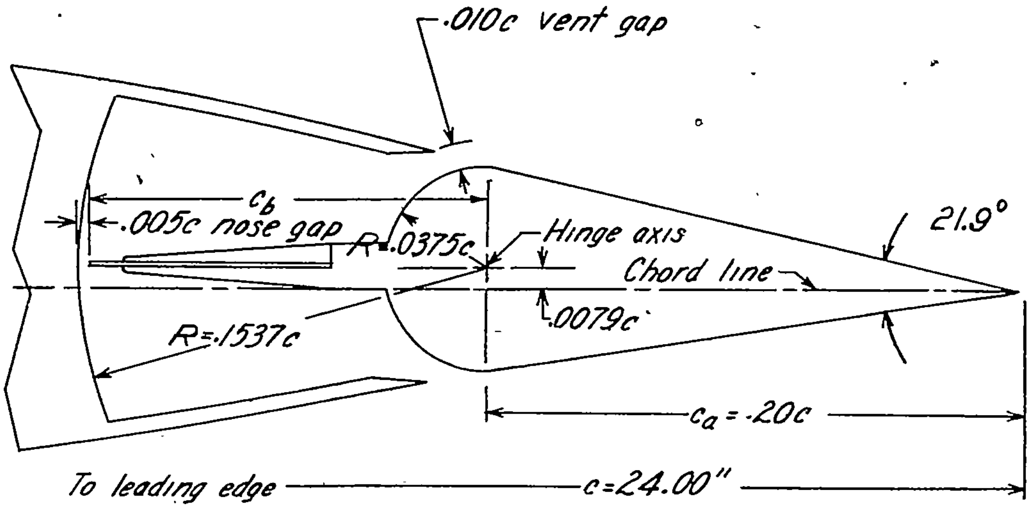

(b) Internally balanced aileron, unsealed.

NATIONAL ADVISORY COMMITTEE FOR AERONAUTICS.

[redacted]

Figure 2. - Straight-sided ailerons tested on NACA 66(215)-216, a=1.0 airfoil section.

UNCLASSIFIED

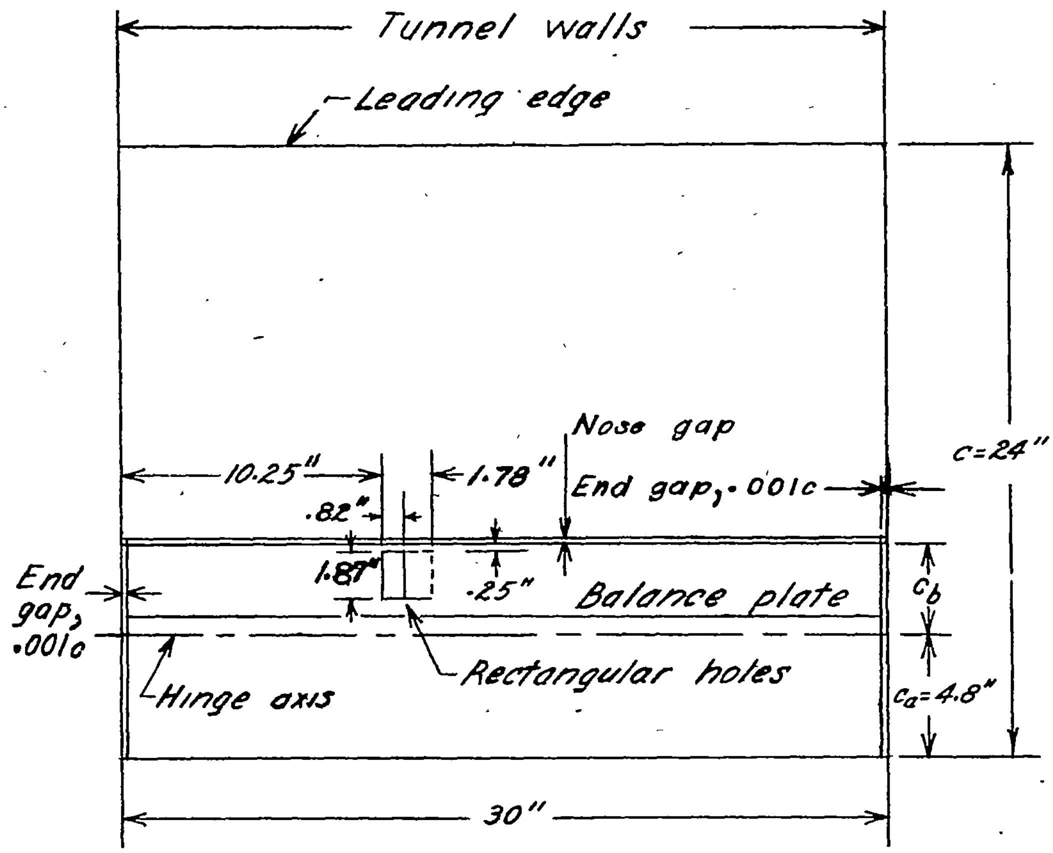

NATIONAL ADVISORY COMMITTEE FOR AERONAUTICS

Figure 3.- Plan view of model with cover plates removed showing locations and sizes of holes cut in balance plate to simulate concentrated leakage.

UNCLASSIFIED

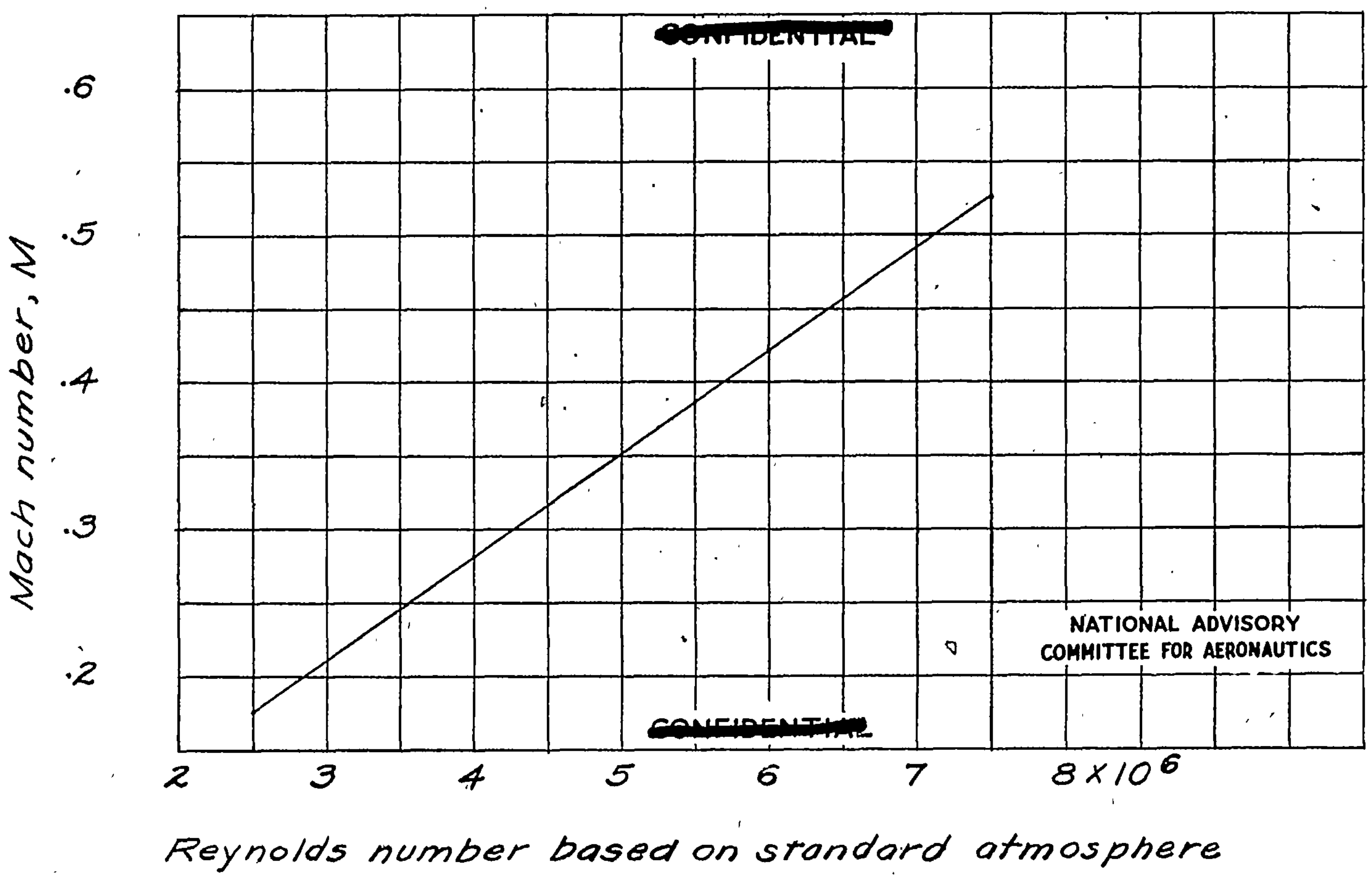

Figure 4.– Reynolds number for values of test Mach number for a 2-foot-chord airfoil in the $2\frac{1}{2}$- by 6-foot test section of the Langley stability tunnel.

UNCLASSIFIED

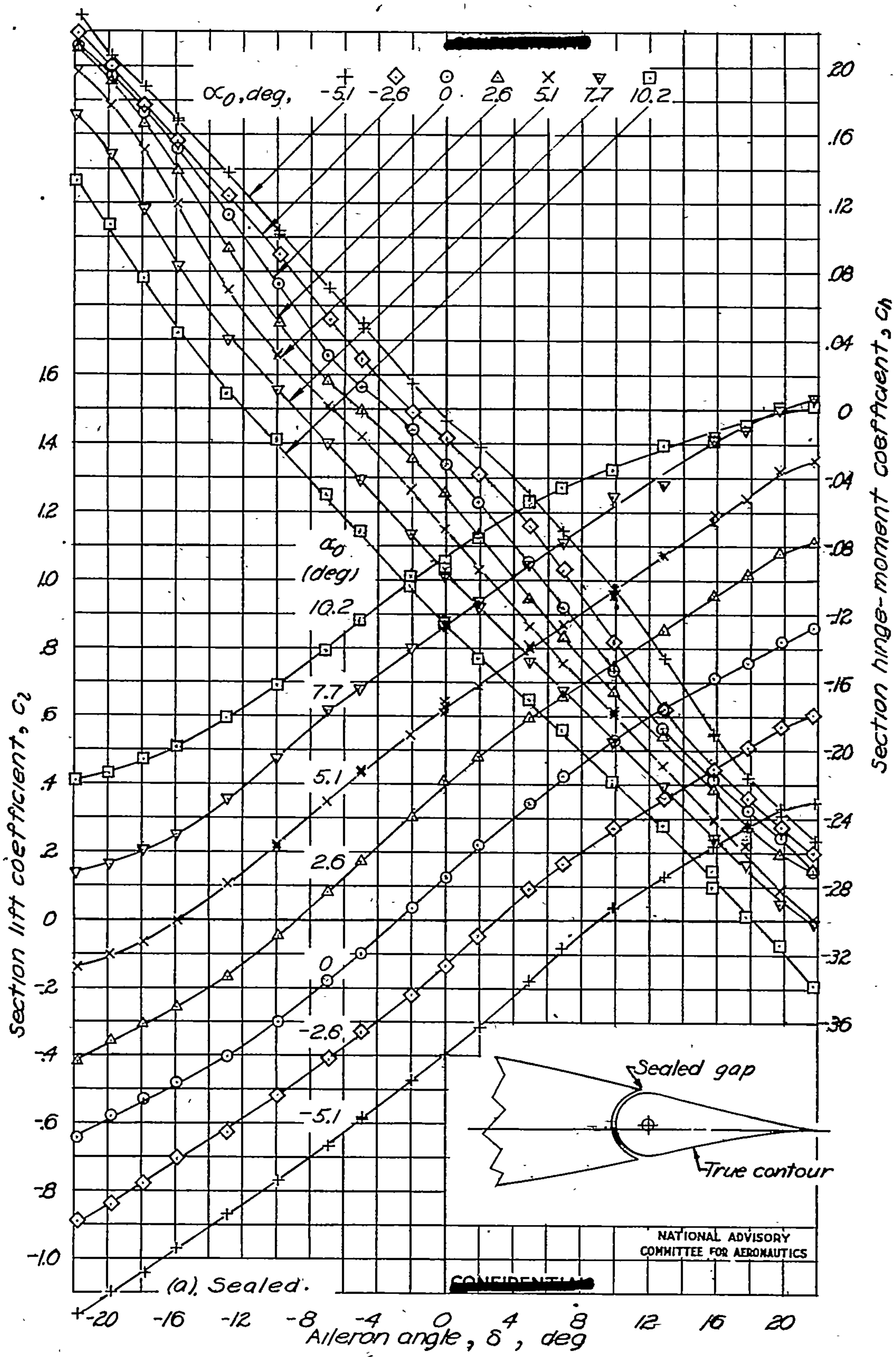

Figure 5.- Variation of section lift and hinge-moment coefficients with aileron angle. True-contour plain aileron; M = 0.36.

UNCLASSIFIED

UNCLASSIFIED

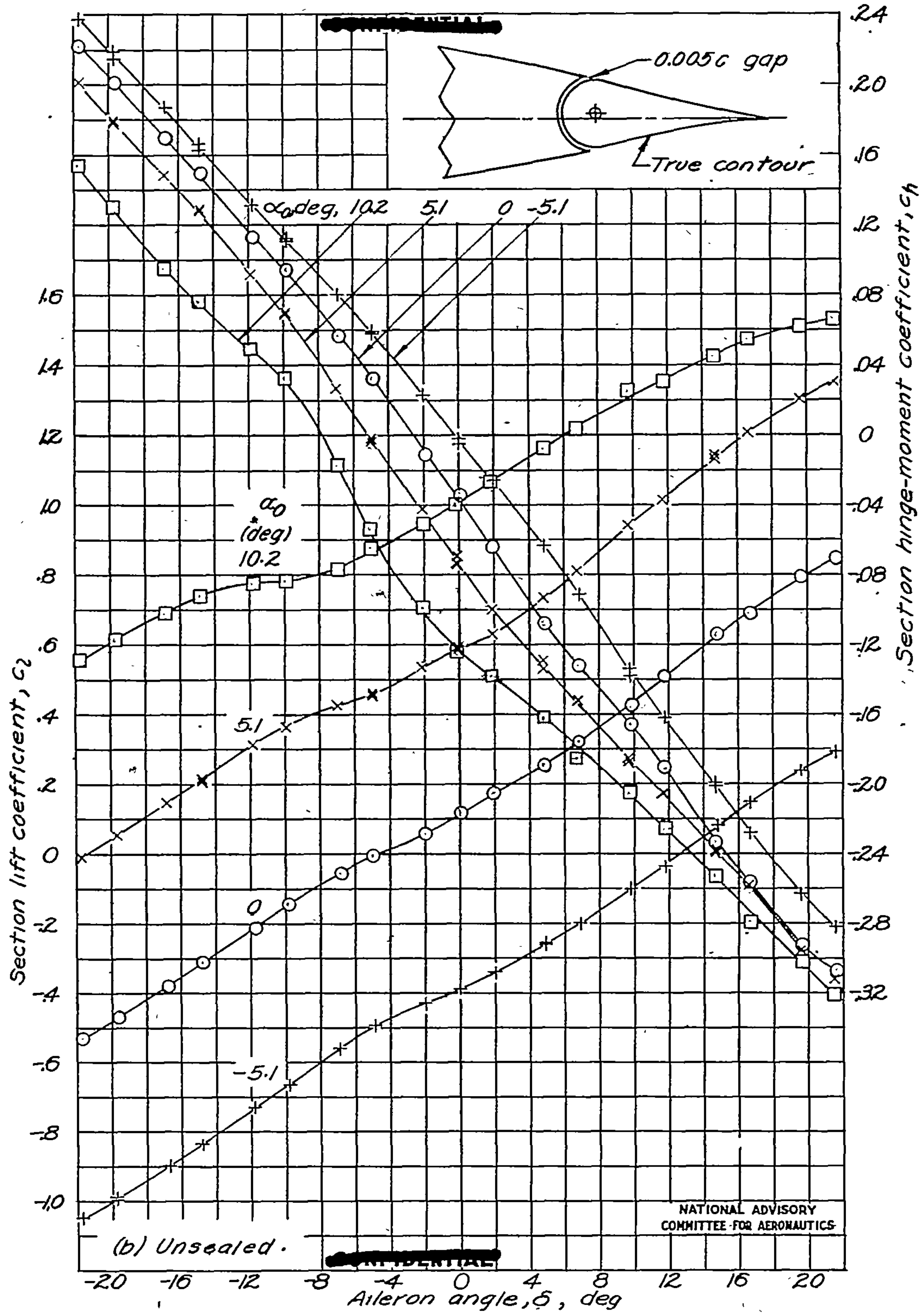

Figure 5. - Concluded.

UNCLASSIFIED

UNCLASSIFIED

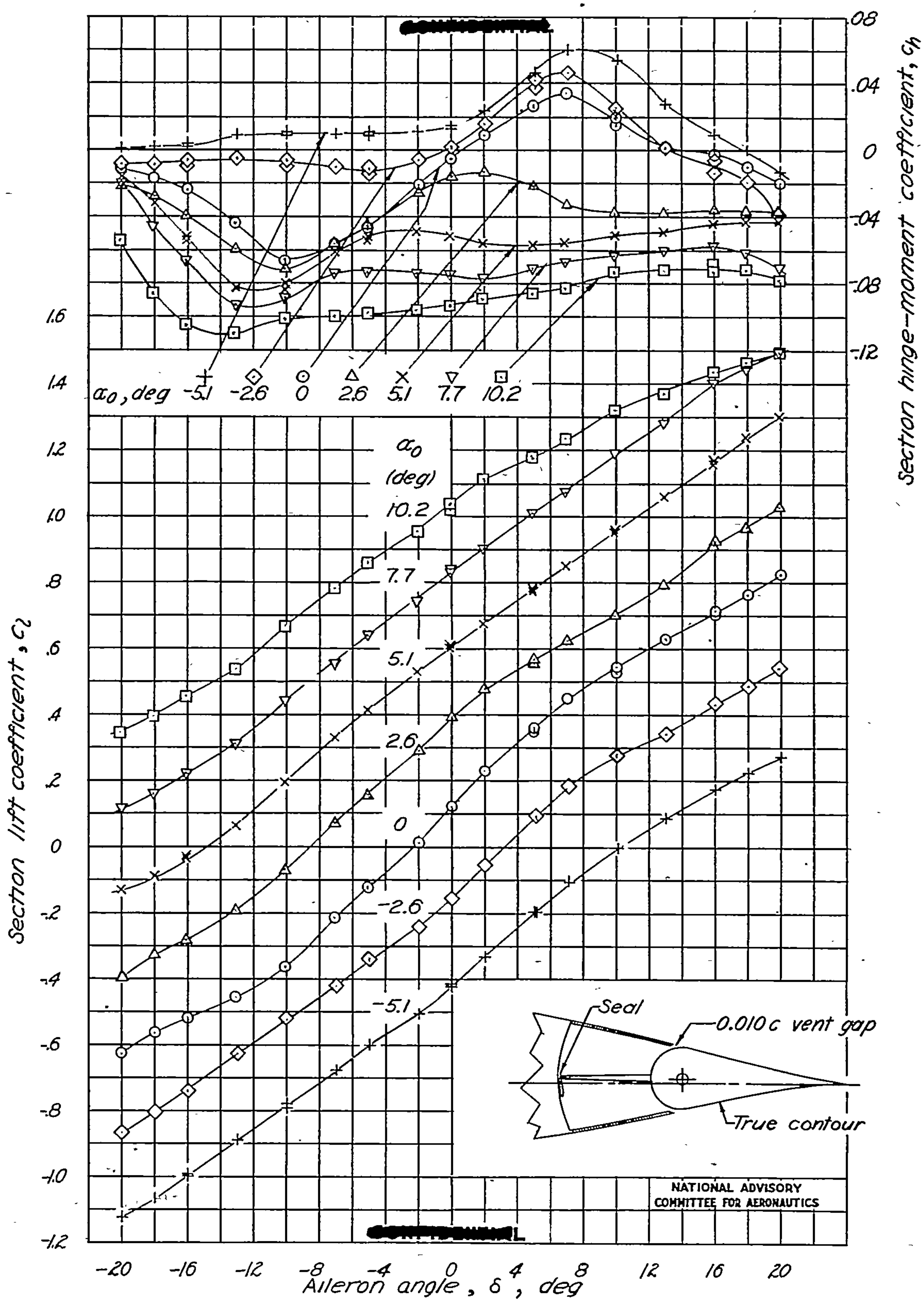

Figure 6.- Variation of section lift and hinge-moment coefficients with aileron angle. True-contour $0.75c_a$ internally balanced aileron ; vent gaps , 0.010c ; end gaps sealed ; nose gap sealed ; M = 0.36.

UNCLASSIFIED

UNCLASSIFIED

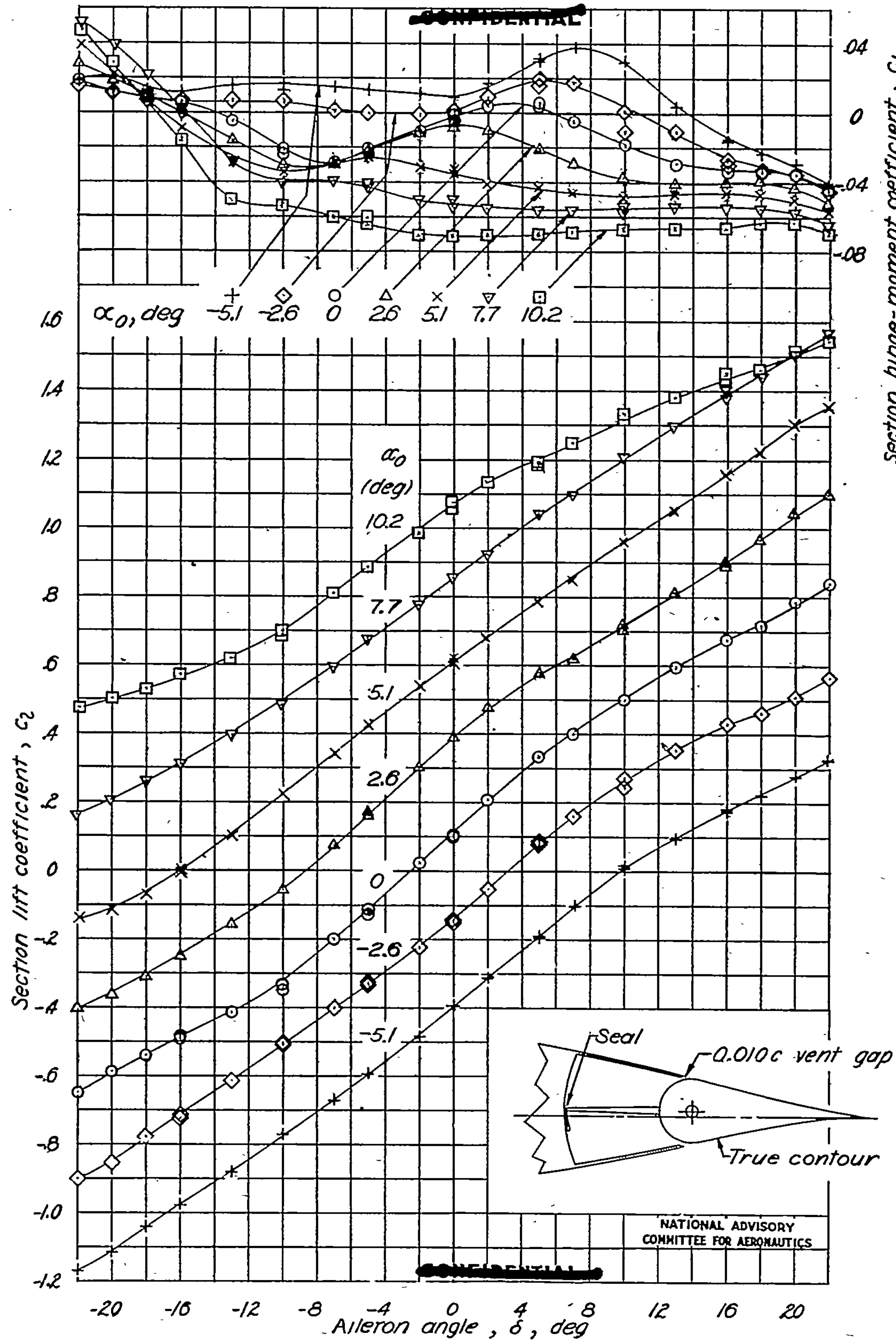

Figure 7.-Variation of section lift and hinge-moment coefficients with aileron angle. True-contour $0.75c_a$ internally balanced aileron; vent gaps, 0.010c; end gaps, 0.001c; nose gap sealed; M = 0.36.

UNCLASSIFIED

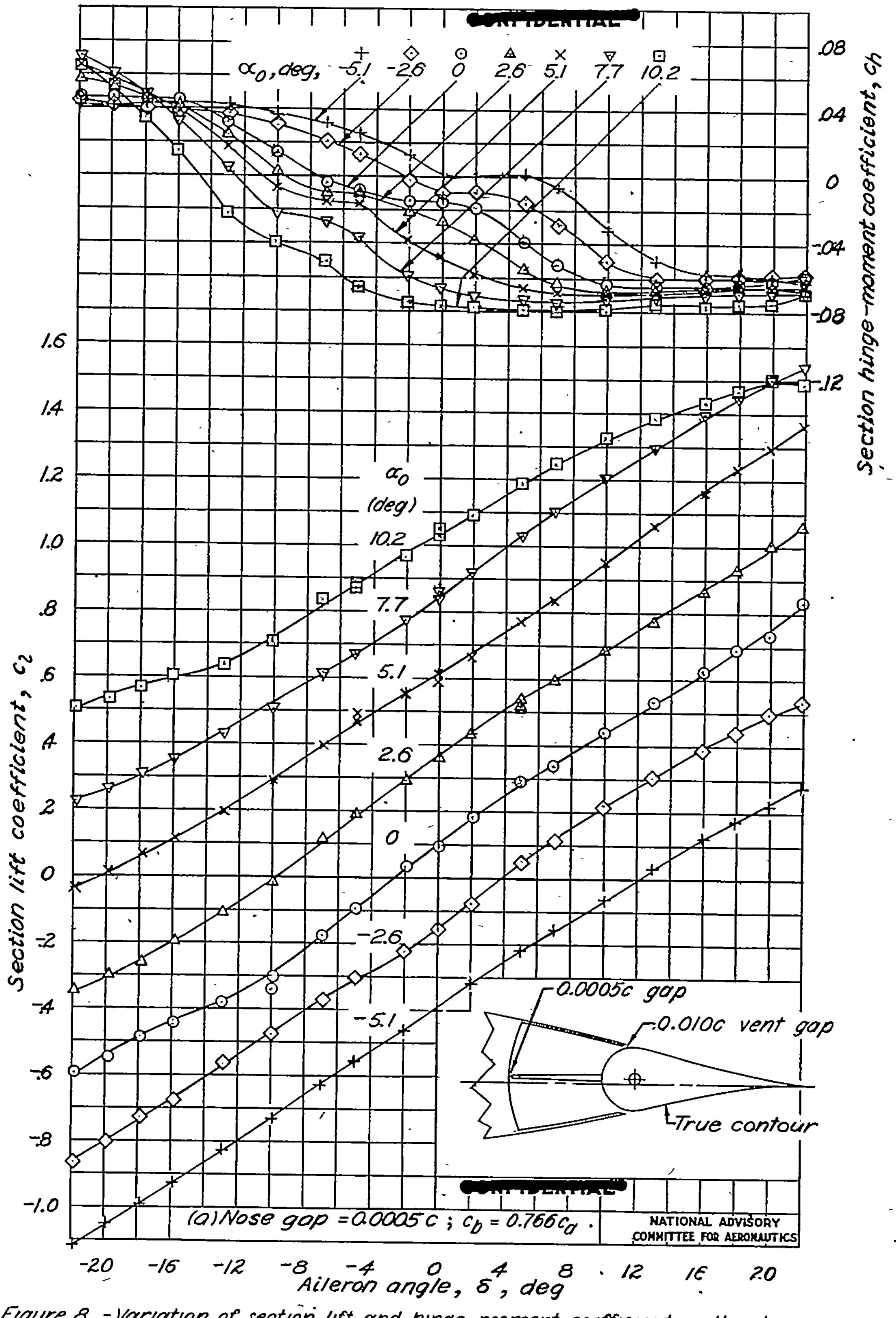

Figure 8.- Variation of section lift and hinge-moment coefficients with aileron angle. True-contour 0.75c_a internally balanced aileron; vent gaps, 0.010c; end gaps, 0.001c; M = 0.36.

UNCLASSIFIED

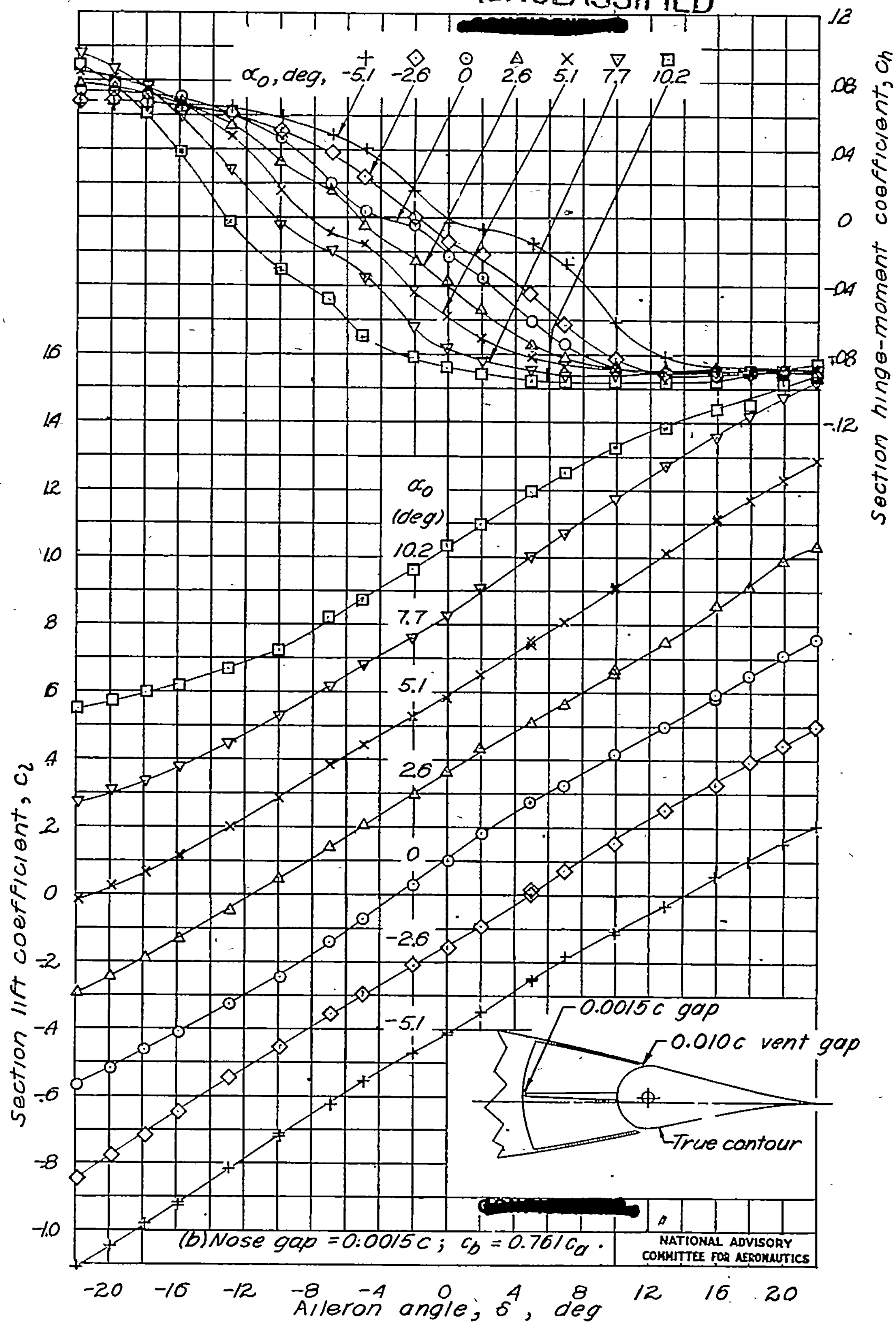

Figure 8.– Continued.

UNCLASSIFIED

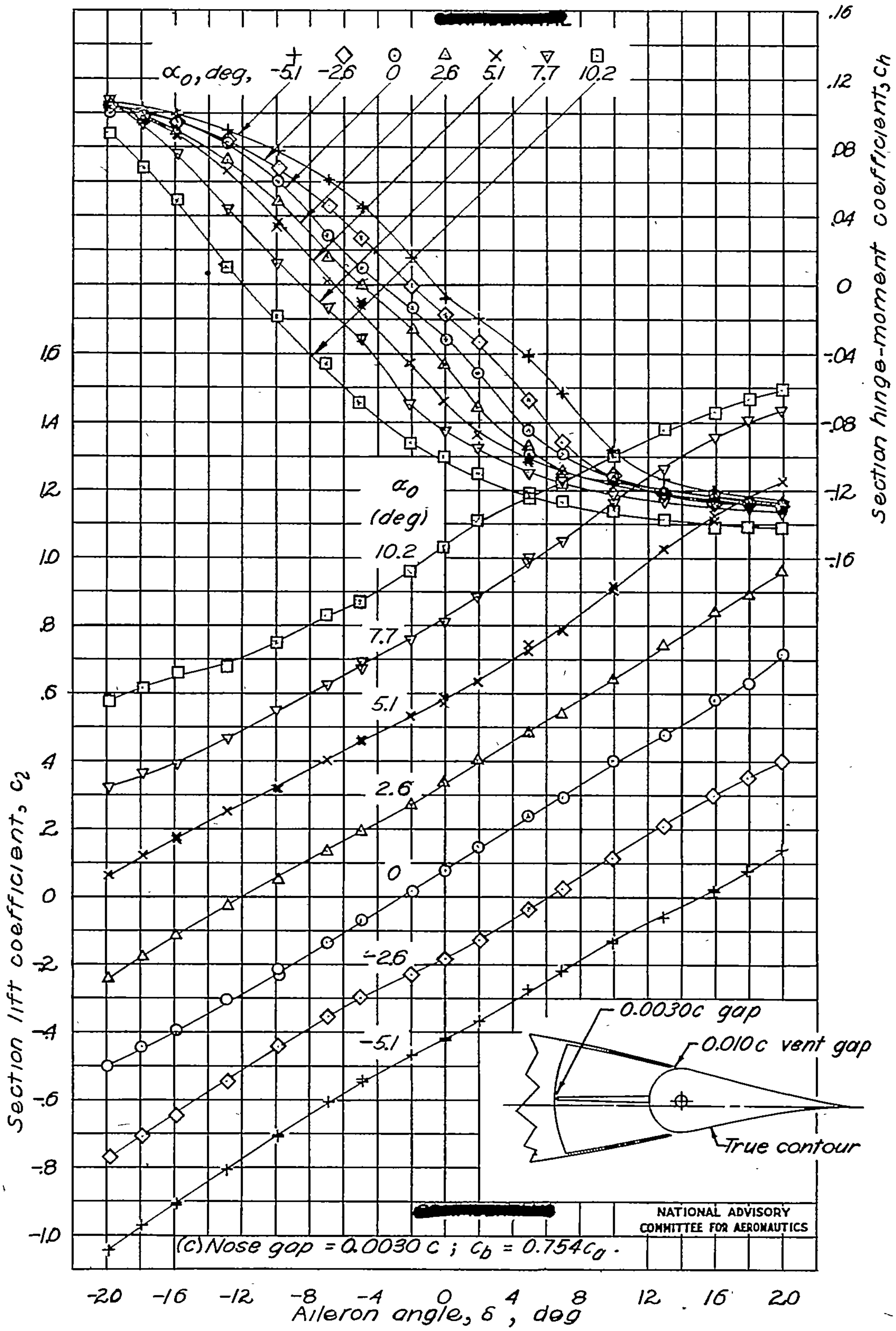

Figure 8- Continued.

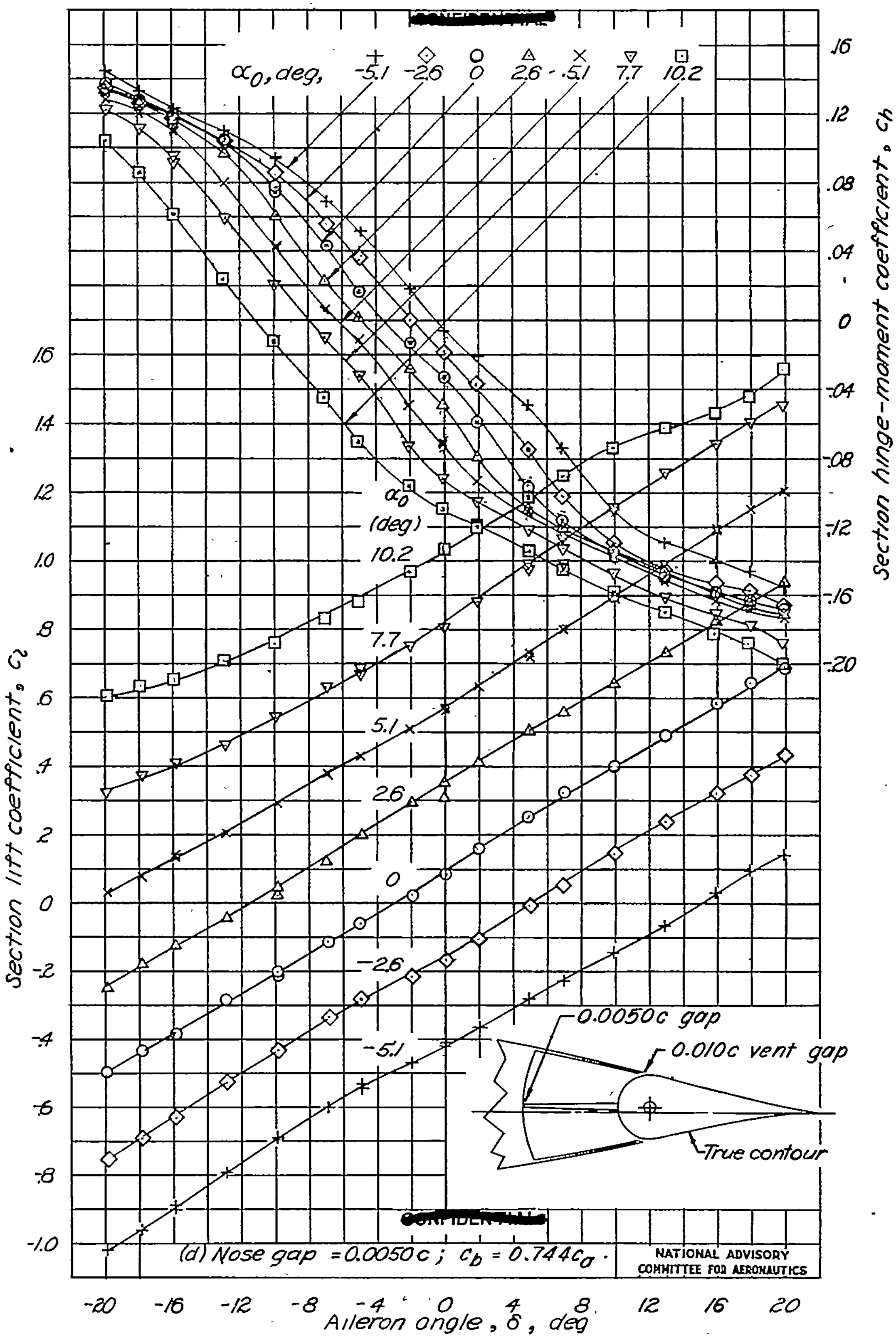

Figure 8.- Continued.

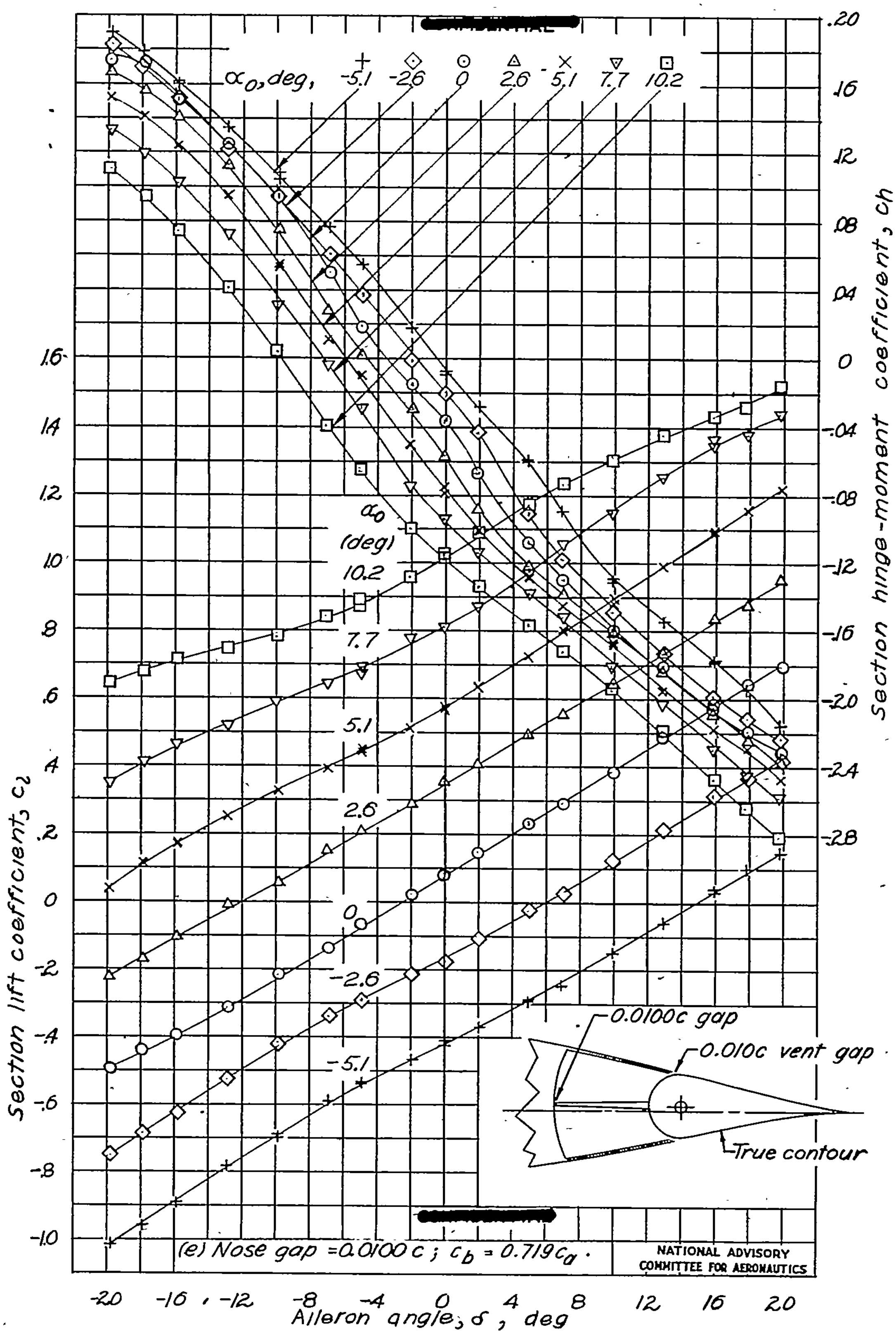

Figure 8.- Concluded.

UNCLASSIFIED

[redacted]

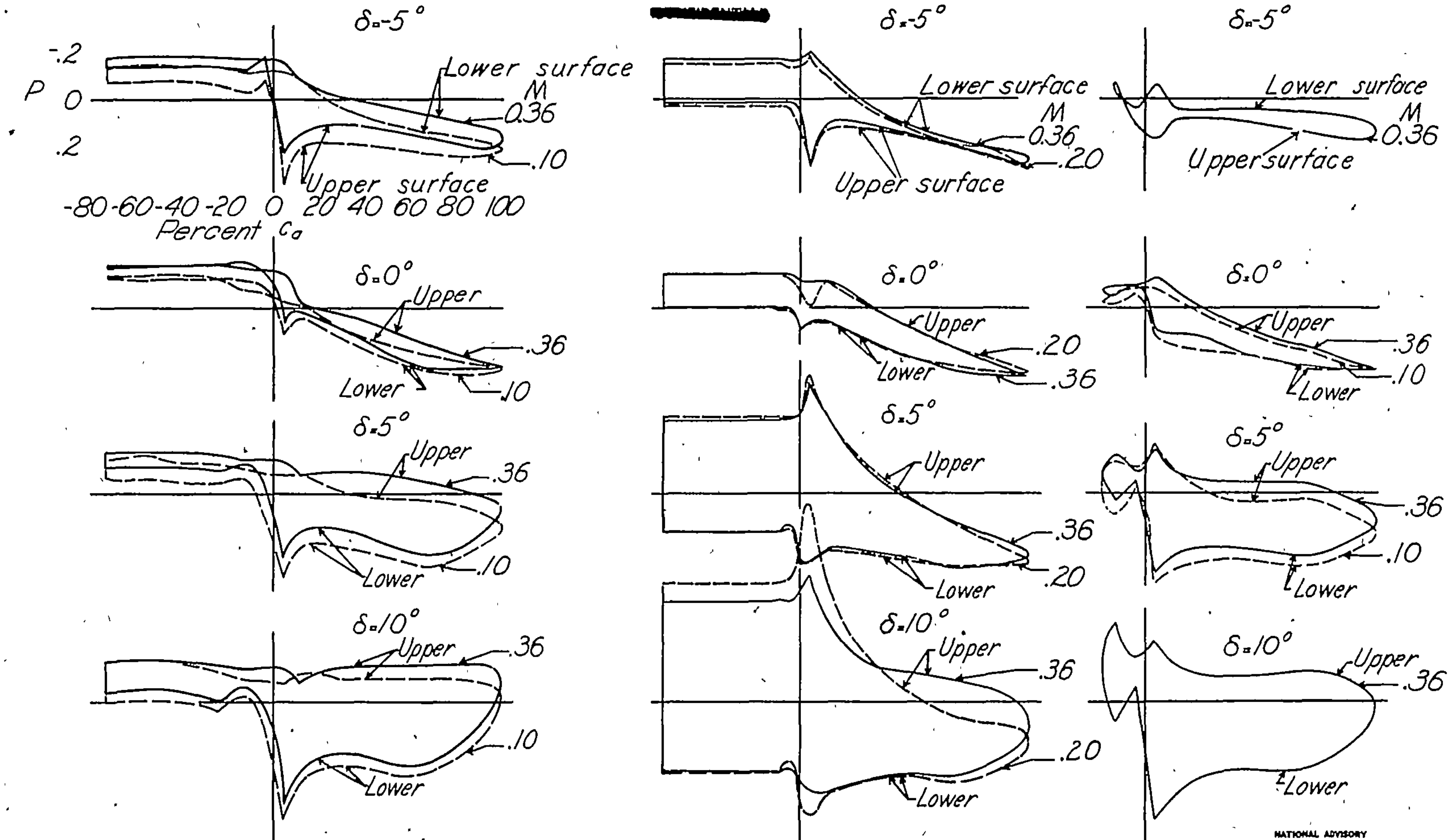

[redacted]

(a) Unsealed internally balanced aileron; nose gap, 0.005 c; vent gaps, 0.010c. (b) Sealed internally balanced aileron; vent gaps, 0.005 c. (c) Plain unsealed aileron; nose gap, 0.005c.

Figure 9.--Pressure distributions over aileron and balance plate. $\alpha_0 = 0°$.

UNCLASSIFIED

[redacted]

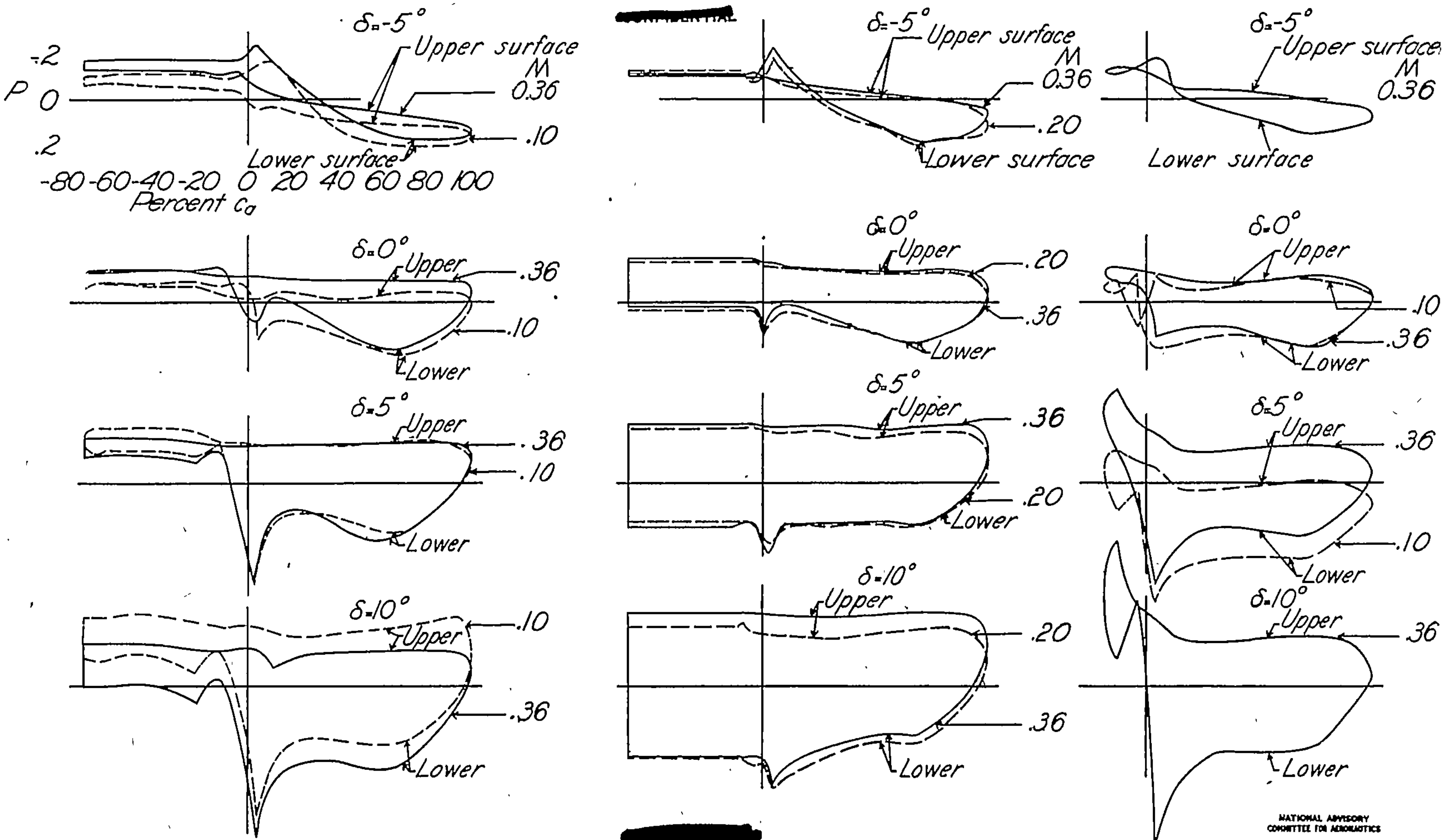

[redacted]

(a) Unsealed internally balanced aileron; nose gap, 0.005c; vent gaps, 0.010c.
(b) Sealed internally balanced aileron; vent gaps, 0.005c.
(c) Plain unsealed aileron; nose gap, 0.005c.

Figure 10.- Pressure distributions over aileron and balance plate. $\alpha_0 = 10°$.

UNCLASSIFIED

[redacted]

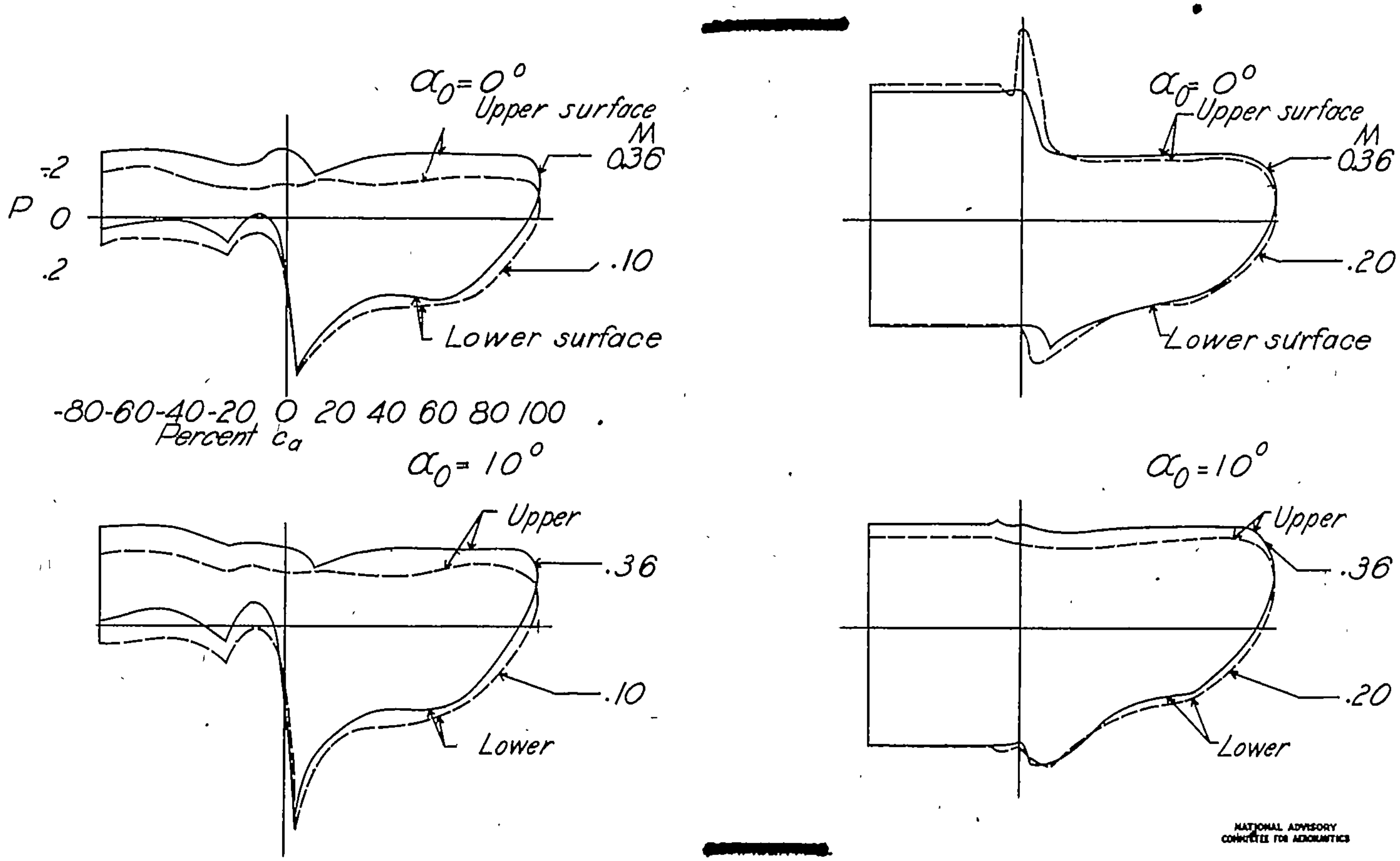

[redacted]

(a) Unsealed internally balanced aileron ; nose gap, 0.005 c ; vent gaps, 0.010 c.

(b) Sealed internally balanced aileron ; vent gaps, 0.005 c.

Figure 11. - Pressure distributions over aileron and balance plate. $\delta = 16°$.

UNCLASSIFIED

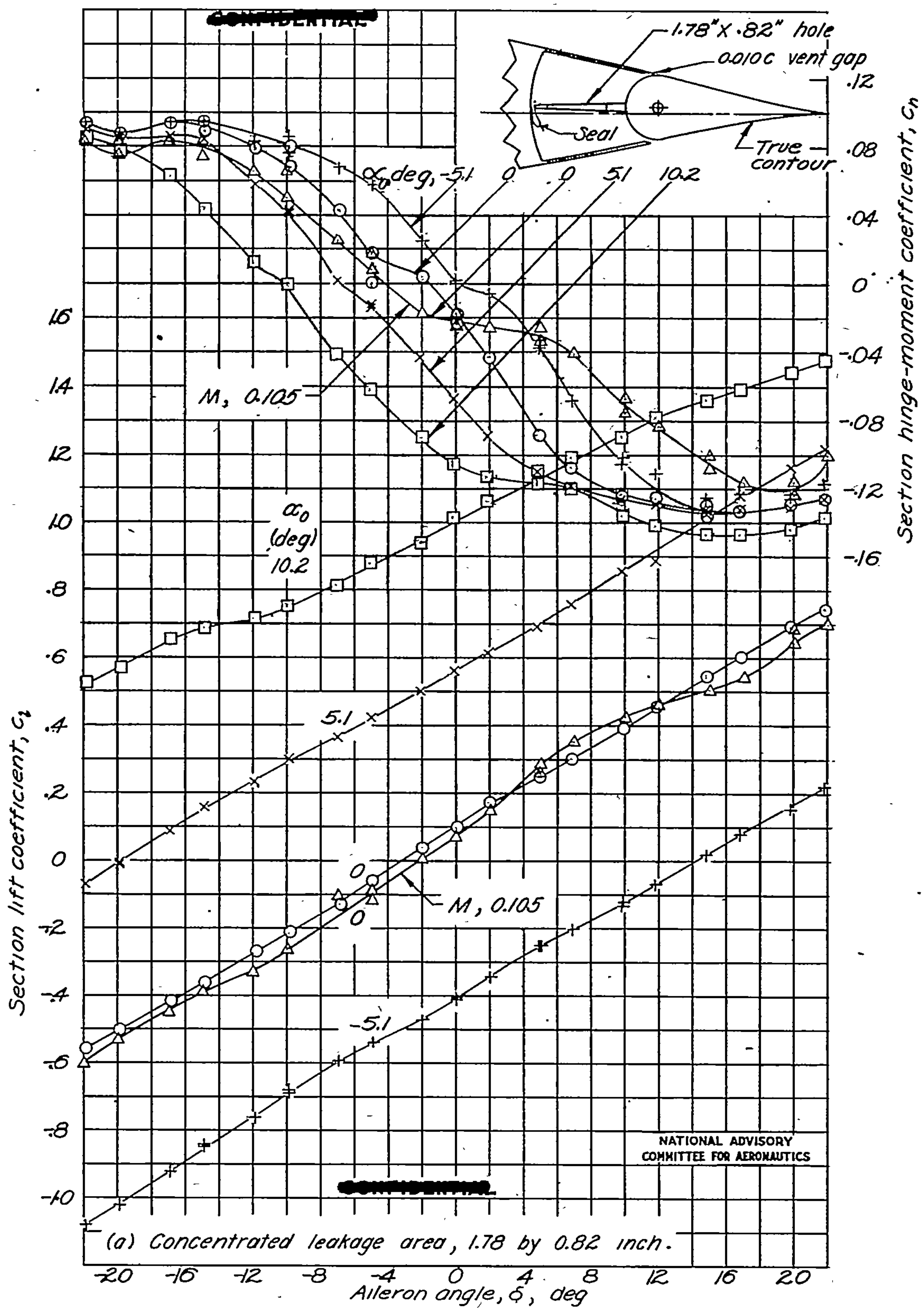

Figure 12.– Variation of section lift and hinge-moment coefficients with aileron angle. True-contour $0.75c_a$ internally balanced aileron with concentrated leakage; vent gaps, 0.010c; end gaps, 0.001c; M = 0.36 except where noted.

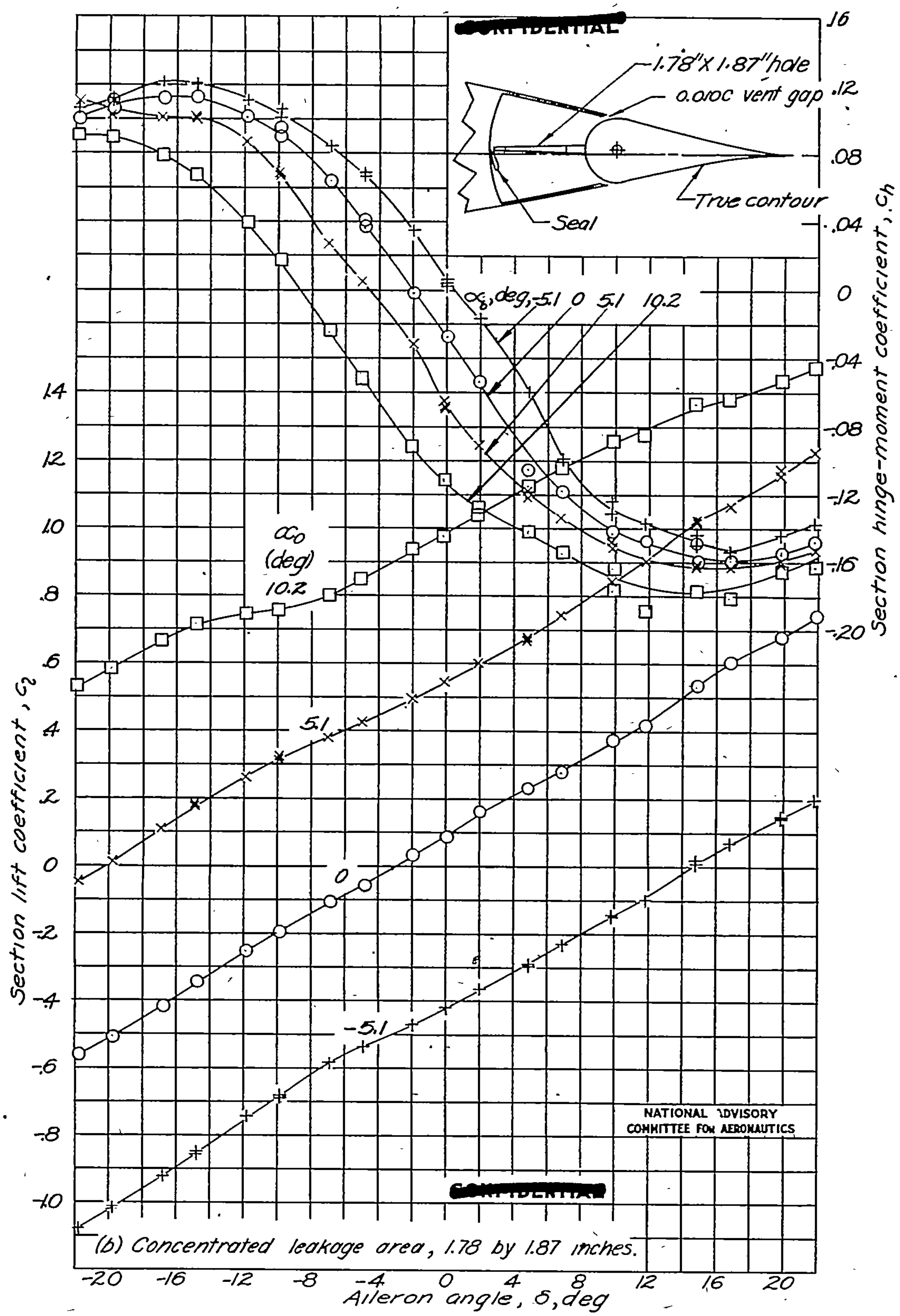

(b) Concentrated leakage area, 1.78 by 1.87 inches.

Figure 12.-Concluded.

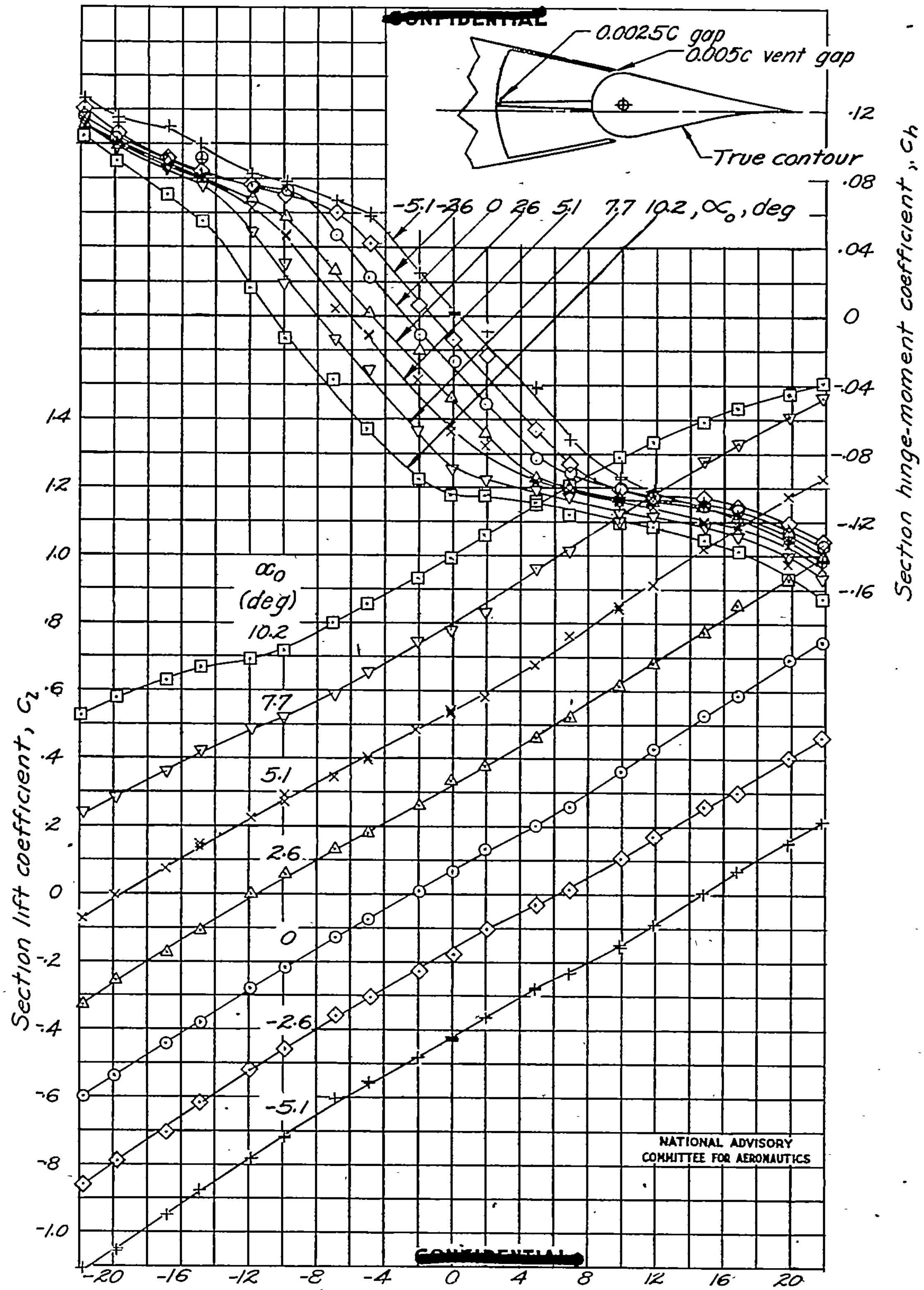

Figure 13.- Variation of section lift and hinge-moment coefficients with aileron angle. True-contour 0.75c_a internally balanced aileron; vent gaps, 0.005c; end gaps, 0.001c; nose gap, 0.0025c; M = 0.36.

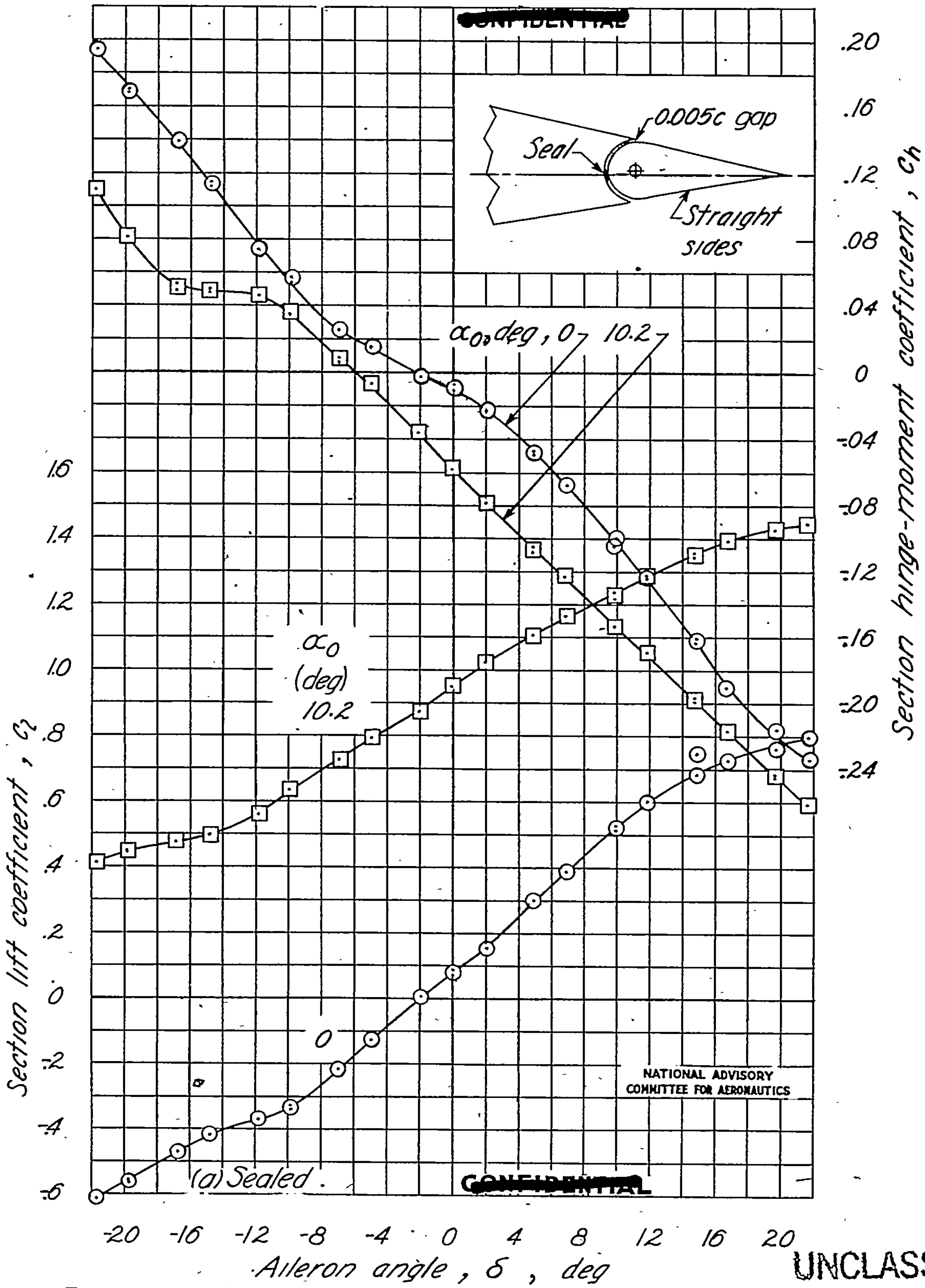

Figure 14.- Variation of section lift and hinge-moment coefficients with aileron angle. Straight-sided plain aileron; nose gap sealed and 0.005c; M = 0.36.

UNCLASSIFIED

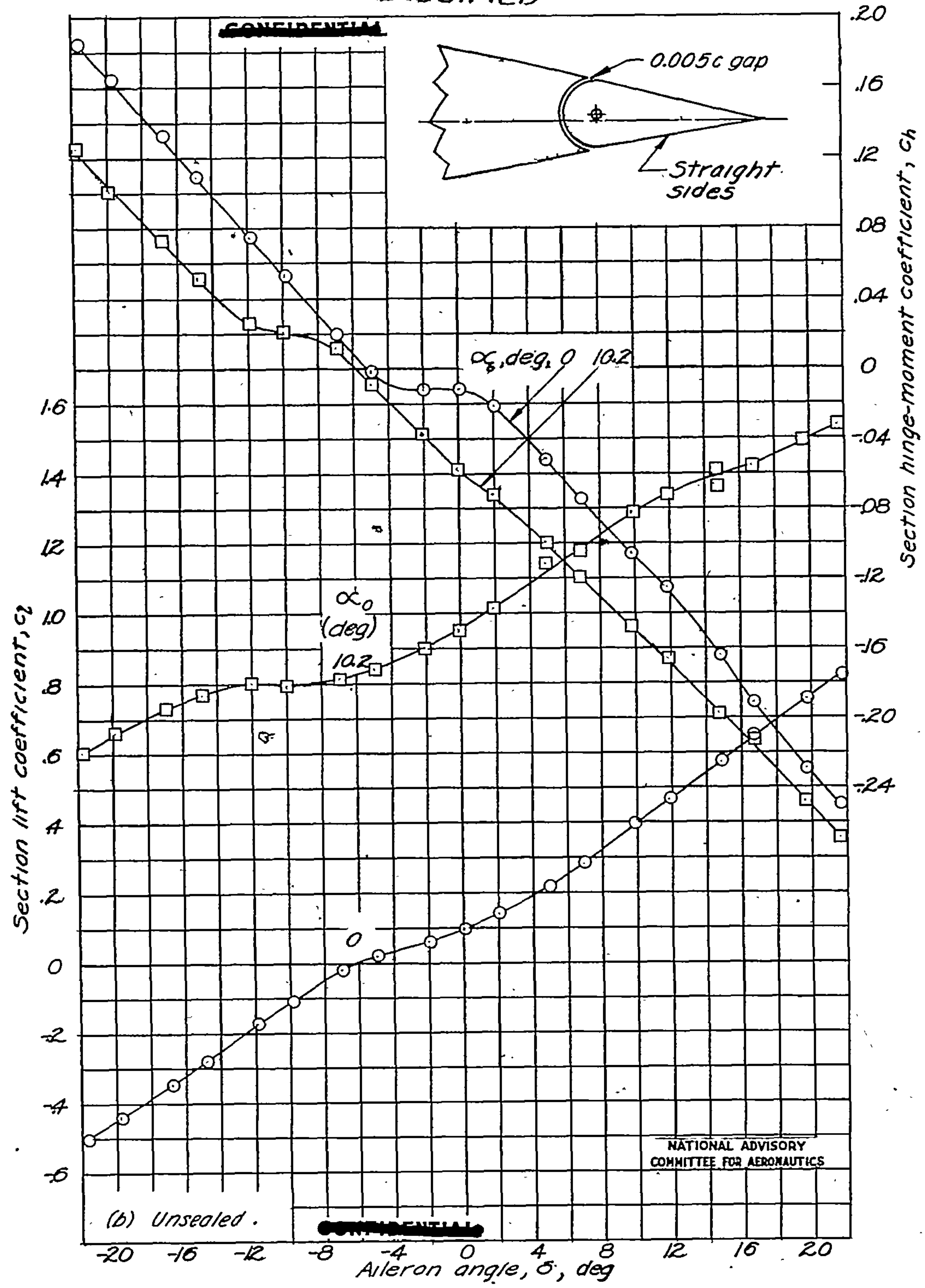

Figure 14.- Concluded.

UNCLASSIFIED

UNCLASSIFIED

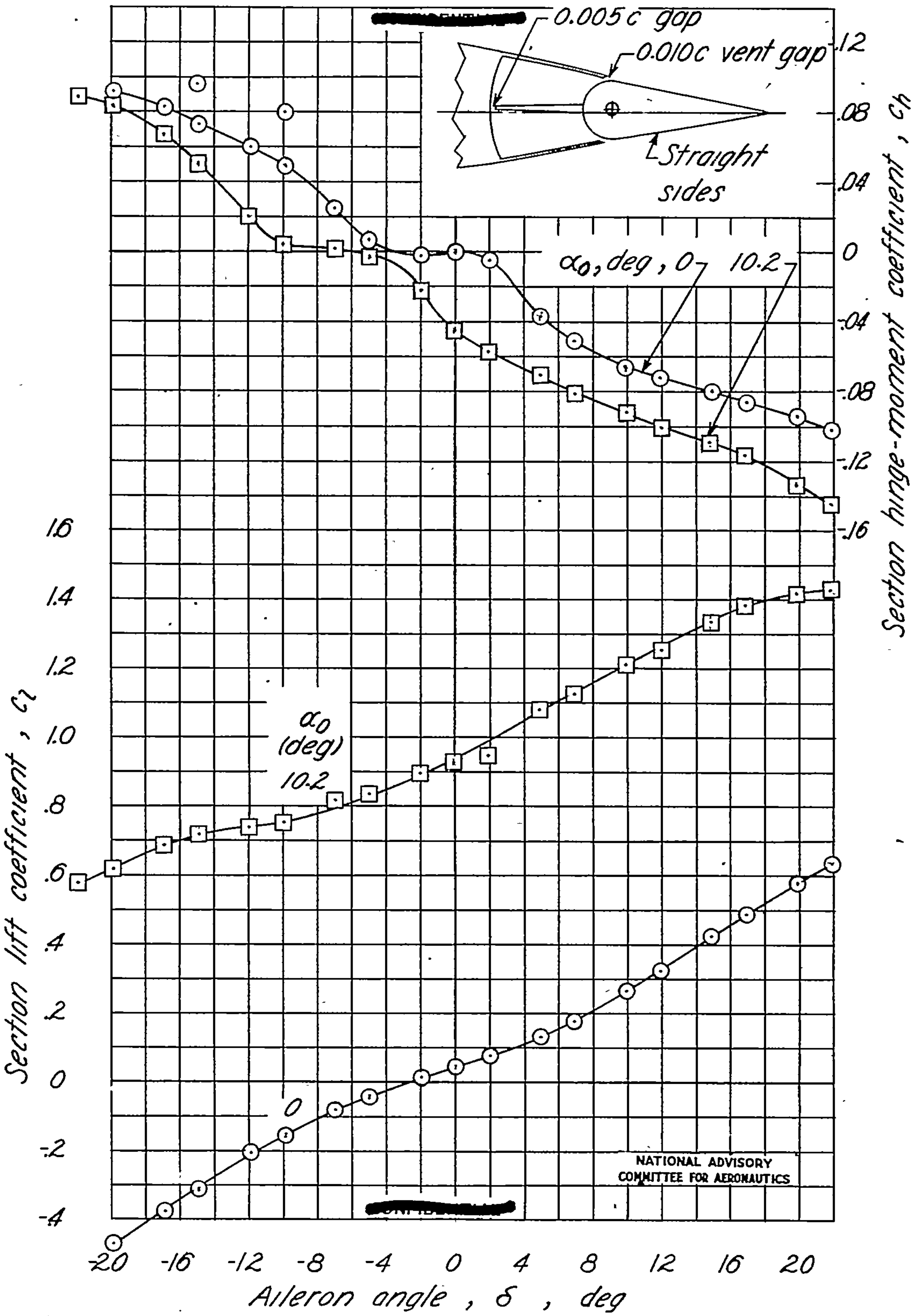

Figure 15.- Variation of section lift and hinge-moment coefficients with aileron angle. Straight-sided $0.75c_a$ internally balanced aileron; vent gaps, 0.010c; end gaps, 0.001c; nose gap, 0.005c; M = 0.36.

UNCLASSIFIED

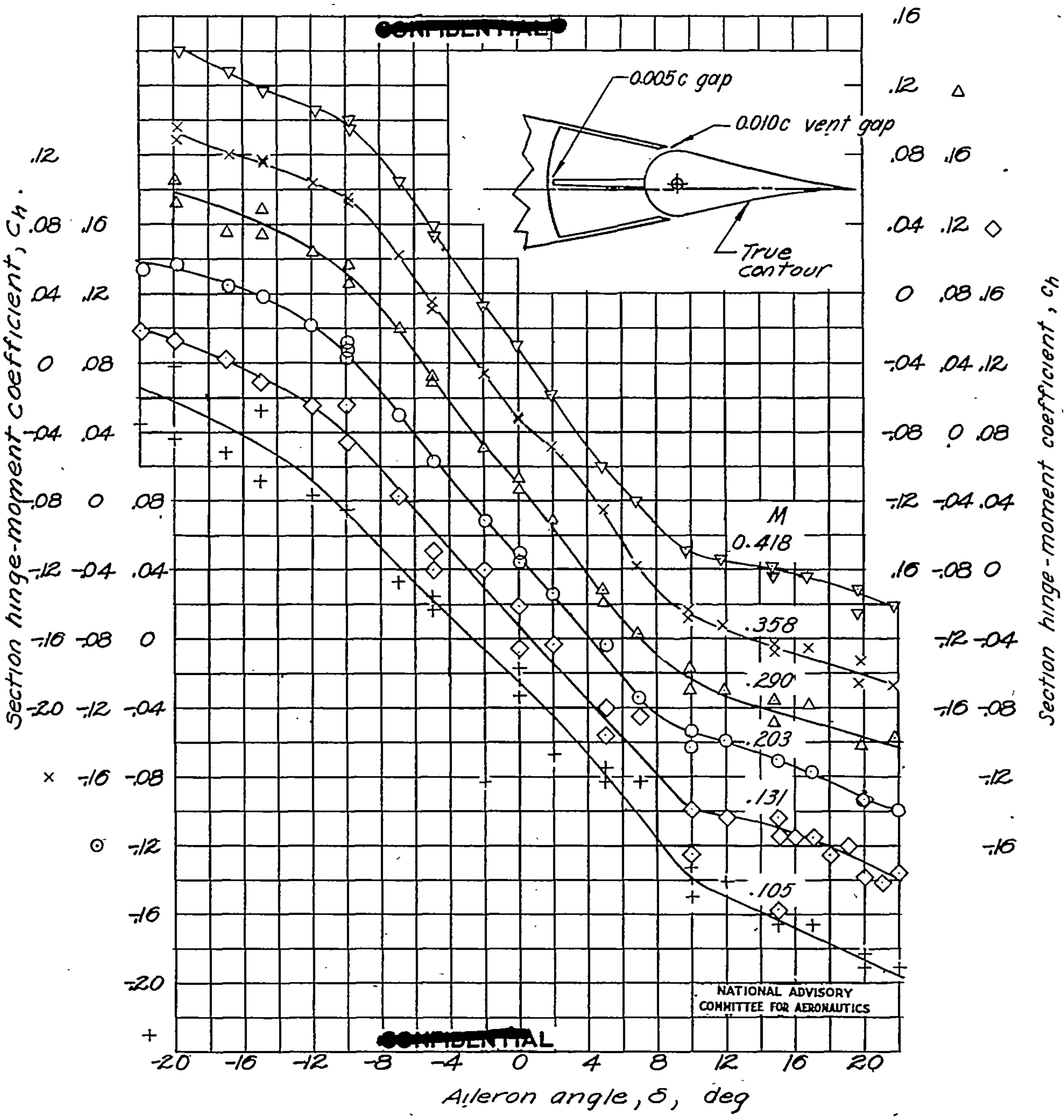

Figure 16.- Effect of Mach number on the variation of hinge-moment coefficient with aileron angle. True-contour $0.75c_a$ internally balanced aileron; vent gaps, 0.010c; end gaps sealed; nose gap, 0.005c; $\alpha_0 = 0°$. (Note staggered scales.)

UNCLASSIFIED

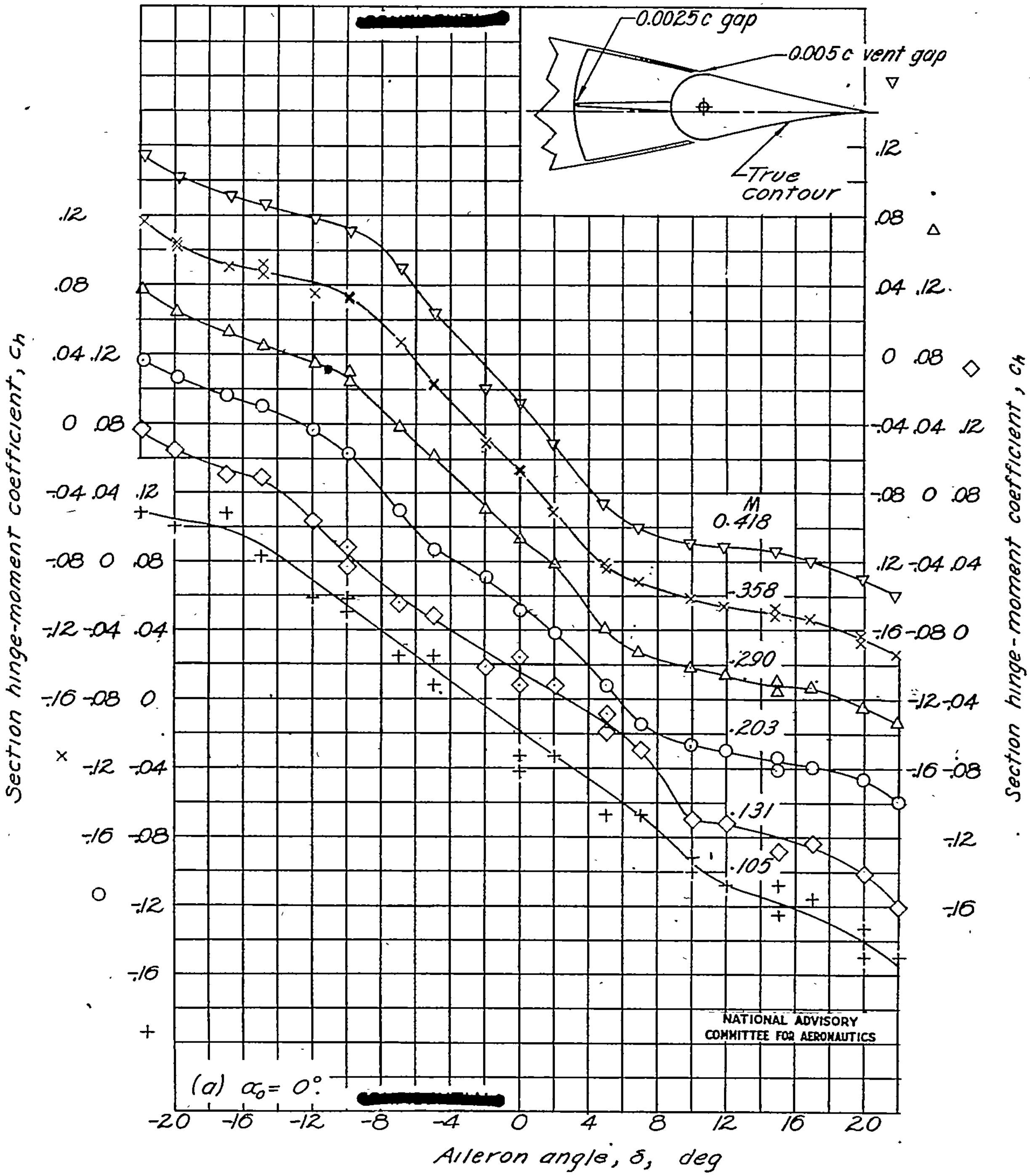

Figure 17.- Effect of Mach number on the variation of hinge-moment coefficient with aileron angle. True-contour $0.75c_a$ internally balanced aileron; vent gaps, 0.005c; end gaps, 0.002c; nose gap, 0.0025c. (Note staggered scales.)

UNCLASSIFIED

UNCLASSIFIED

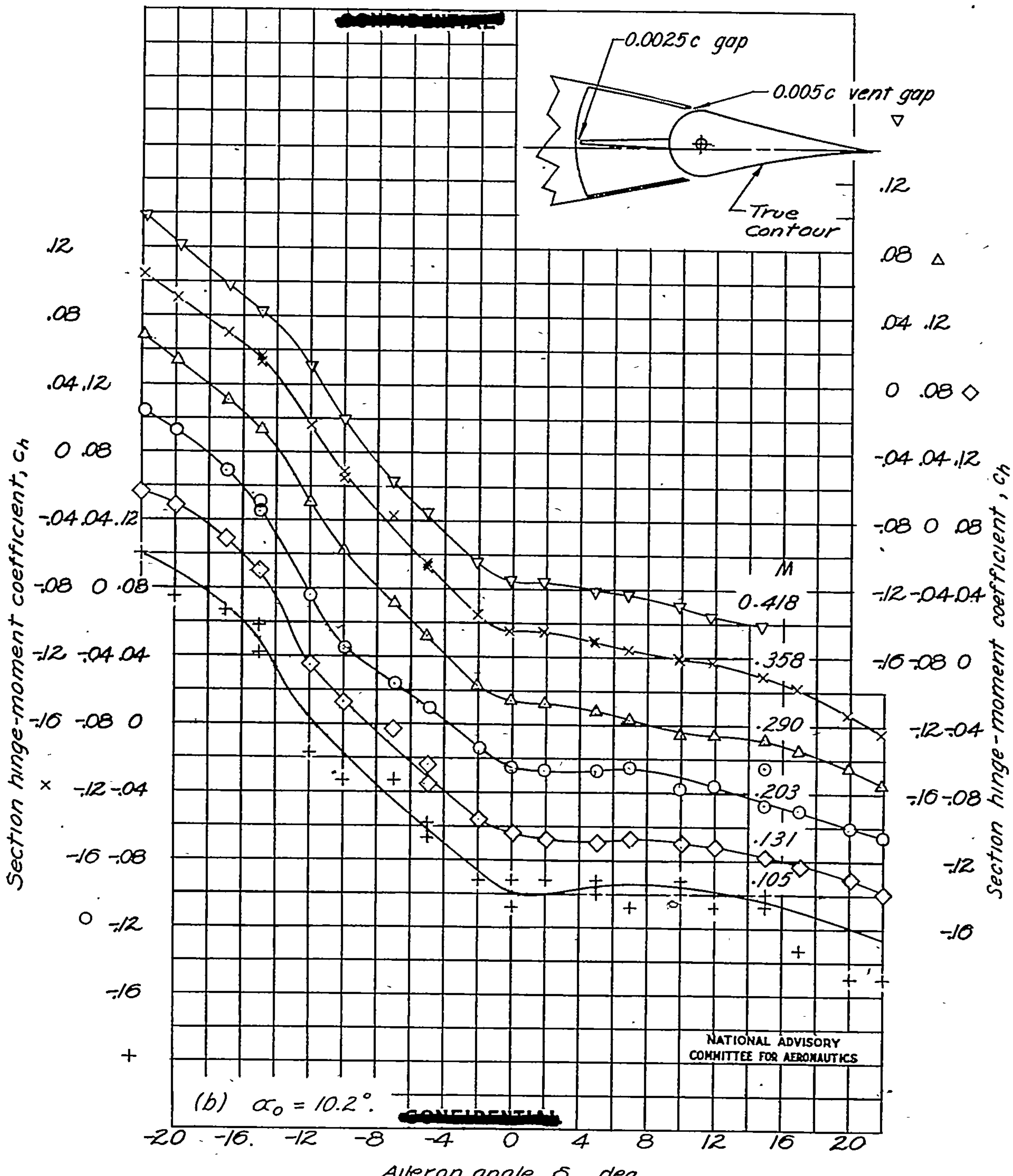

Figure 17.-Concluded.

UNCLASSIFIED

[redacted]

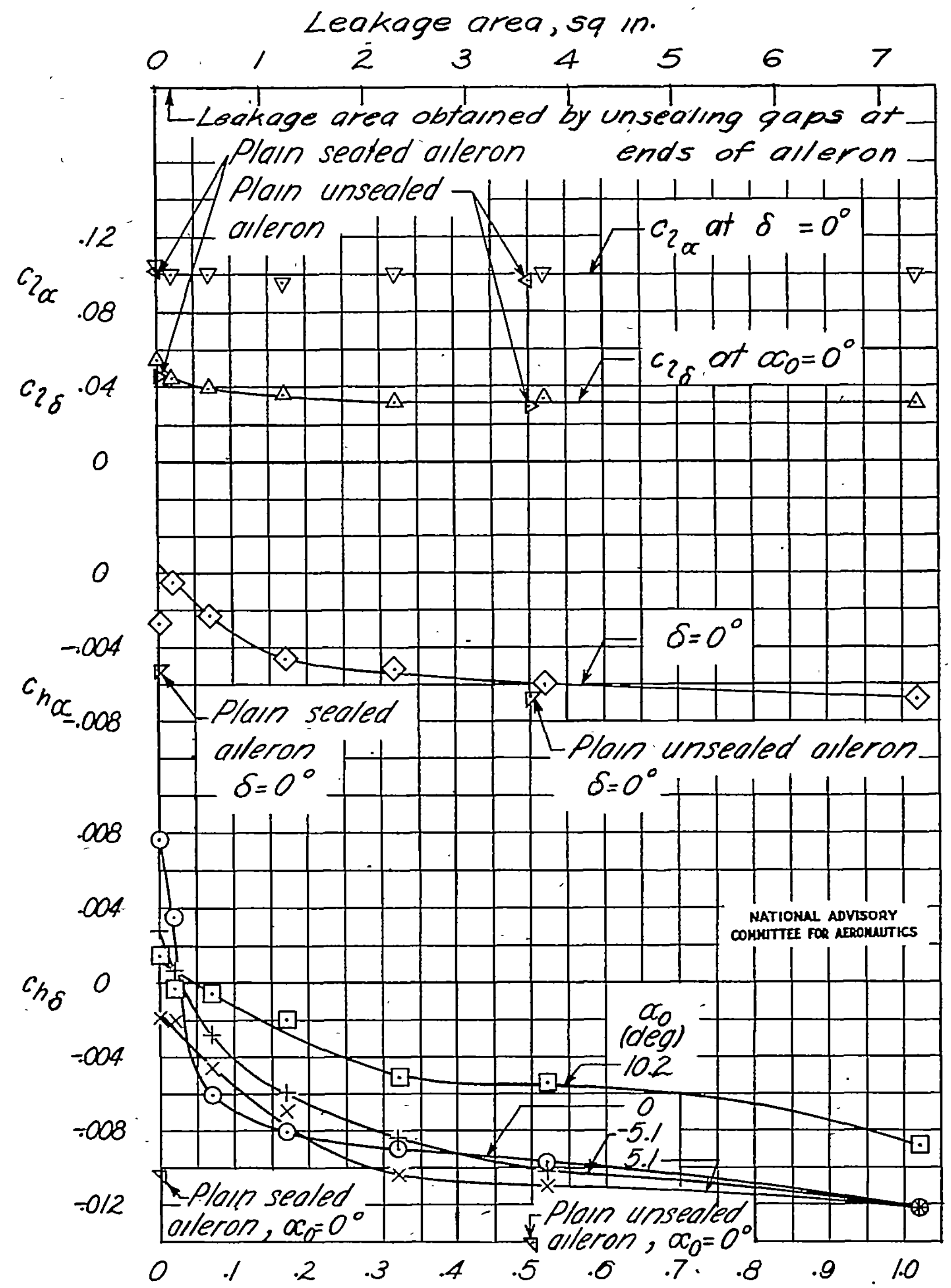

Figure 18.- Variation of lift and hinge-moment parameters with leakage area; true-contour plain aileron and true-contour $0.75c_a$ internally balanced aileron with 0.010c vent gaps; $M = 0.36$.

[redacted]

UNCLASSIFIED

UNCLASSIFIED

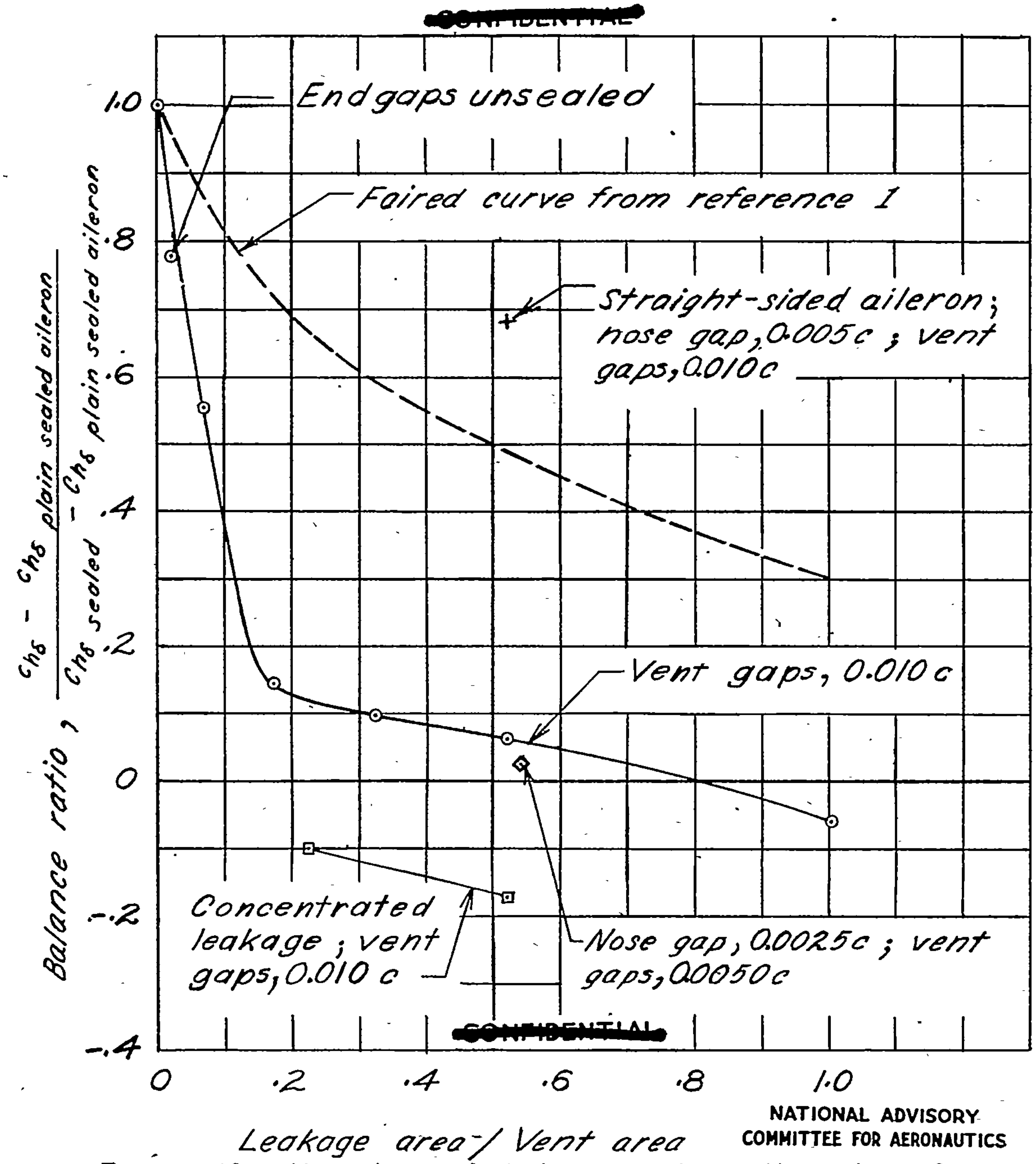

Figure 19.- Variation of balance ratio with ratio of leakage area to vent area; balance ratio computed by using c_{h_δ} of plain sealed aileron; $M = 0.36$; $\alpha_0 = 0°$.

UNCLASSIFIED

UNCLASSIFIED

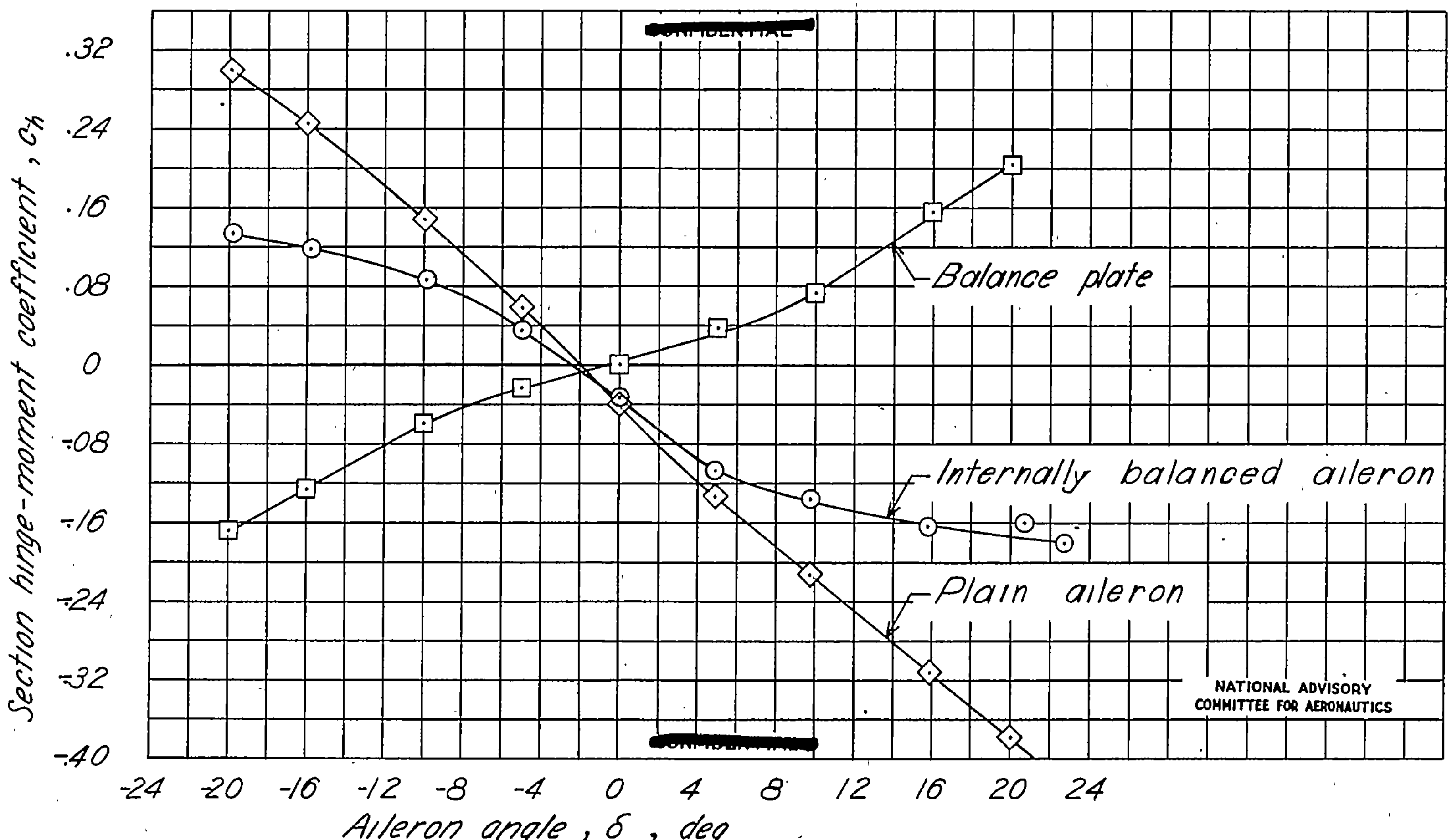

Figure 20.- Variation of section hinge-moment coefficient with aileron angle (from pressure distributions). True-contour 0.75c_a internally balanced aileron; vent gaps, 0.010c; end gaps sealed; nose gap, 0.005c; M = 0.36; α_0 = 0°.

UNCLASSIFIED

UNCLASSIFIED

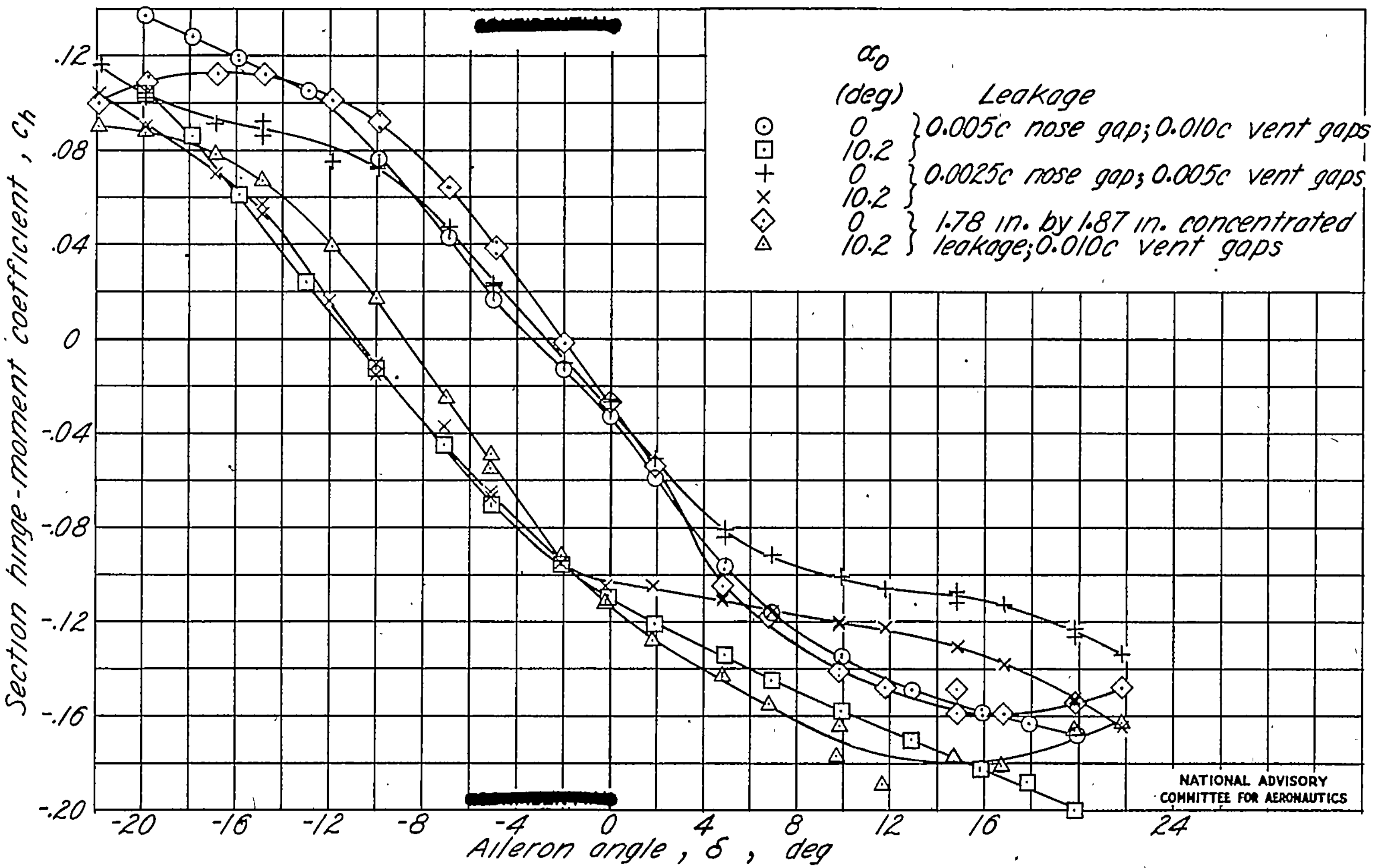

Figure 21.- Characteristics of true-contour $0.75c_a$ internally balanced ailerons having approximately a constant ratio of leakage area to vent area of 0.5; M = 0.36. All end gaps, 0.001c.

UNCLASSIFIED

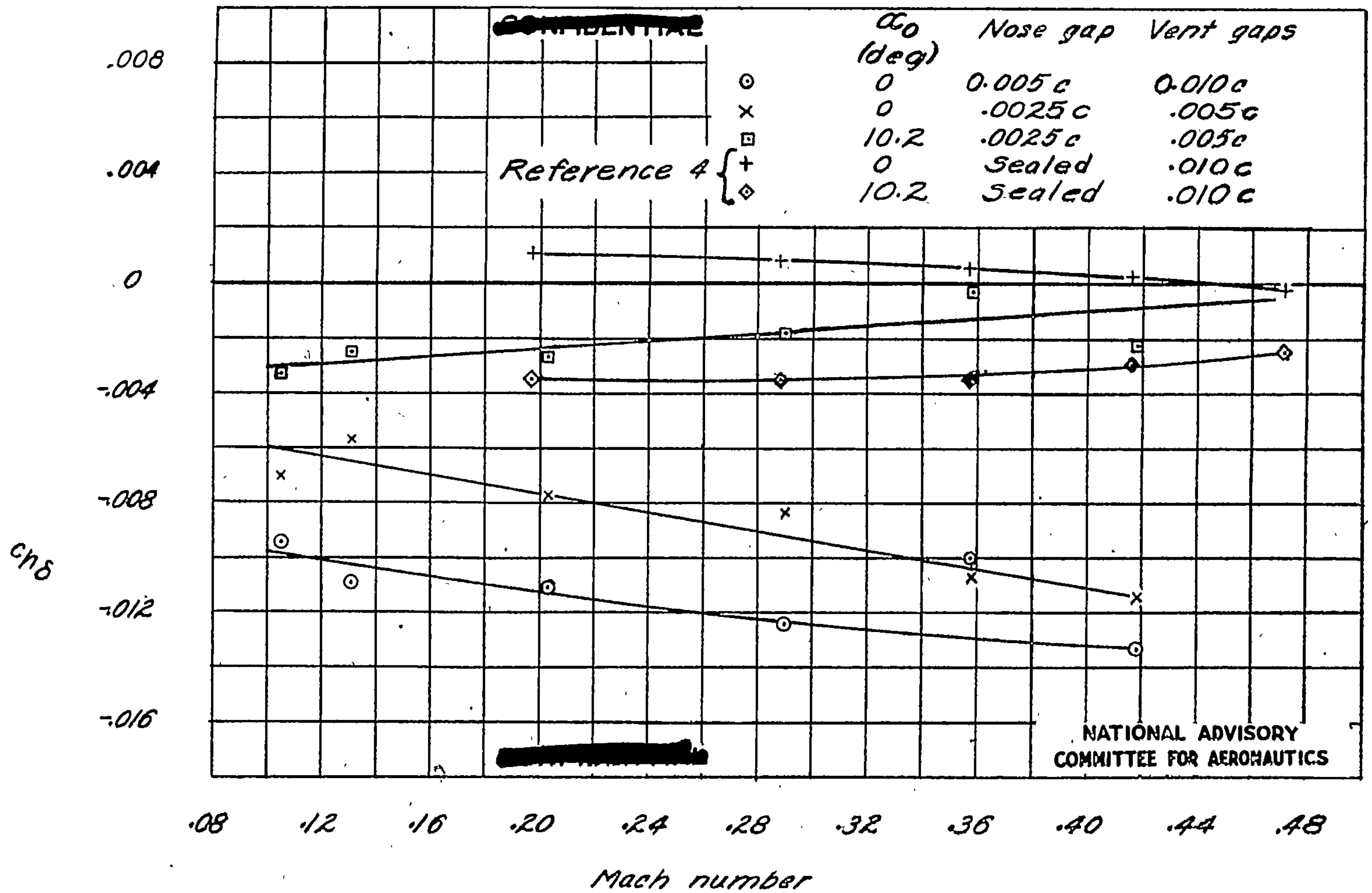

Figure 22.- Variation of c_{h_δ} with Mach number. True-contour $0.75c_a$ internally balanced aileron; data from figures 11 and 12 and reference 4.